Available online at www.sciencedirect.com
SCIENCE DIRECT®
Atomic Data and Nuclear Data Tables 92 (2006) 375–406
Atomic Data AND Nuclear Data Tables
www.elsevier.com/locate/adt

Analytic cross sections for electron impact collisions with nitrogen molecules

Tatsuo Tabata [a,b], Toshizo Shirai [c,⁂], Masao Sataka [d], Hirotaka Kubo [c,*]

[a] *Osaka Prefecture University, Gakuen-cho, Sakai, Osaka 599-8531, Japan*
[b] *Institute for Data Evaluation and Analysis, Kami, Sakai, Osaka 593-8311, Japan*
[c] *Department of Fusion Plasma Research, Japan Atomic Energy Research Institute, Naka-shi, Ibaraki 319-0193, Japan*
[d] *Department of Materials Science, Japan Atomic Energy Research Institute, Tokai-mura, Ibaraki 319-1195, Japan*

Abstract

Cross sections for 74 processes in collisions of electrons with nitrogen molecules (N_2) and singly ionized nitrogen molecules (N_2^+) have been collected. The literature has been surveyed through the middle of 2004. The data sets collected are presented in separate graphs for each process. Recommended cross sections are expressed by analytic expressions.

* Corresponding author. Fax: +81 0 29 270 7419.
E-mail address: kubo.hirotaka@jaea.go.jp (H. Kubo).
⁂ Deceased.

0092-640X/$ - see front matter © 2006 Elsevier Inc. All rights reserved.
doi:10.1016/j.adt.2006.02.002

Contents

1. Introduction

Cross section data on collision processes of electrons with nitrogen molecules (N_2) and singly ionized nitrogen molecules (N_2^+) are important in studying low-temperature plasmas in nature and industrial techniques of gaseous electronics and plasma processing. In the field of thermonuclear fusion research, the use of N_2, Ne, Ar, and other gases is being studied. The deliberate introduction of these impurities is intended to solve the problems of reducing the peak power loads and erosion of diverter components to acceptable levels. Thus, this also makes the accurate knowledge of the above data a necessity. The latest review of these data were included in articles by Trajmar et al. [1], Itikawa et al. [2], and Majeed and Strickland [3]. Trajmar et al. surveyed experimental techniques for measuring electron-molecule cross sections and available experimental data on electron scattering by various molecules including N_2, and numerically presented recommended cross sections applying renormalization when necessary. Itikawa et al. graphically gave recommended cross sections for collisions of electrons and photons with N_2. Majeed and Strickland numerically reported surveyed sets of total ionization and excitation cross sections of electrons in collisions with N_2, O_2, and O. Bibliographies of low-energy electron cross section data are included in [4–8]. Hayashi [9] published an extensive bibliography of original and review reports on experiments and theories of electron collisions with N_2 covering the period 1906–2000.

In the present work, we have updated the compilation of cross sections for collisions of electrons with N_2 and have made a new compilation of cross sections for collisions of electrons with (N_2^+) surveying the literature through the middle of 2004. Threshold phenomena, resonances, dissociative attachment, and coincidence measurements are not covered in the present compilation. To facilitate dissemination of numerical data for practical applications we present the recommended data in the form of analytic expressions obtained by least-squares fits to the collected data. In evaluating the recommended data, no general criteria for the screening of data have been applied, but considerations for rejecting some data points or data sets are described individually in the next subsection. This work has been done as part of the work at Japan Atomic Energy Research Institute to expand the Japanese Evaluated Atomic and Molecular Data Library (JEAMDL; http://www-jt60.naka.jaeri.go.jp/JEAMDL/index.html) (see [10,11] for the latest work).

1.1. Data sources

1.1.1. The Nitrogen molecule (N_2)

The total cross section (Graph 1) was measured by Nickel et al. [12] in the energy range 4–300 eV within a total error of 4.1%, by Nishimura and Yano [13] in the 7–500 eV range within a statistical error of 19%, by Hoffman et al. [14] in the 2.2–700 eV range within a statistical uncertainty of 3%, by Brennan et al. [15] from the integration of differential cross sections measured by a crossed-beam technique in the 1.5–5.0 eV range within an overall uncertainty of 25%, and by Garcia et al. [16] in the 600 eV–5 keV range within an error of 3%. The method used by Nickel et al. [12], Nishimura and Yano, Hoffman et al., and Garcia et al. is a beam attenuation technique. Itikawa et al. [2] gave a recommended data set in the energy range 0.05 eV–5 keV by revising the earlier recommendation by Hayashi [17]. The present compilation also includes the data set of Itikawa et al. All the data sets are quite consistent. The total cross section has fine structure around the 2.3-eV shape resonance, but this structure has been smoothed out in the present treatment. The same also applies to the fine structure in other cross sections.

Data on the elastic scattering cross section (Graph 2) are available from Brennan et al. [15] in the energy range 1.5–

5.0 eV and Shi et al. [18] at energies of 0.55 and 1.5 eV. The latter authors used the integration of differential cross sections measured by the relative flow technique, and the standard deviation of the results are ±6%. We have also used the recommended data of Itikawa et al. [2] obtained in the 0.05–2 keV range revising the earlier recommendation by Hayashi [17]. All the data sets are consistent.

The data for the momentum transfer cross section (0.01 eV–3.4 keV) (Graph 3), and the cross section for rotational excitation of $J = 0 \rightarrow 2$ (0.03–3 eV) (Graph 4) were also taken from the recommendation by Itikawa et al. While the former is the revision of Hayashi's recommendation [17], the latter is based on Onda's calculation [19].

The cross section for vibrational excitation for $v = 0 \rightarrow 1$ (Graph 5) has been taken from Itikawa et al. [2] in the energy range 1–50 eV. The cross sections for vibrational excitation for $v = 0 \rightarrow 2$ and for $v = 0 \rightarrow 3$ (Graphs 6 and 7) were measured by Brennan et al. [15] at energies 2.1 and 3.0 eV and by Sweeney and Shyn [20] by a crossed-beam technique in the energy range 1.9–2.6 eV within a total error of about 20%. Sweeney and Shyn also measured the cross section for vibrational excitation for $v = 0 \rightarrow 4$ (Graph 8) in the 2.1–2.6 eV range. The energy range in which the last three cross sections are available are so narrow that we have not made analytic expressions for those cross sections. We have used the compilation by Majeed and Strickland [3] for the total vibrational excitation cross section (Graph 9; here "total" means sum over final vibrational states) in the 1.3–6 eV range. To make an analytic expression for this cross section, the contributions of vibrational excitation for $v = 0 \rightarrow 1$ at lower and higher energies (Graph 5) have been taken into account.

Cross sections for excitation to the triplet states $A^3\Sigma_u^+$, $B^3\Pi_g$, $W^3\Delta_u$, and $B'^3\Sigma_u^-$ and the singlet states $a'^1\Sigma_u^-$, $a^1\Pi_g$, and $w^1\Delta_u$ (Graphs 10–16) in the energy range from around 10 to 50 eV were taken from recommendations by Trajmar et al. [1], and those in the energy range from threshold to 200 or 1 keV, from Majeed and Strickland [3]. The former authors applied renormalization to original data, when necessary, to take into account newer N_2 elastic scattering cross sections. The two recommendations agree well in the overlapping energy range. Recently Campbell et al. [21] reported values for all these cross sections in the energy range from 15 to 50 eV. They obtained those values from the earlier crossed-beam differential cross section measurements of their group. While being roughly in agreement with the two sets of recommendations, the data points of Campbell et al. show rather large scatter. Therefore, we have not used them for determining the parameters of analytic expressions, though they are shown in the graphs of the present compilation. The results of Finn and Doering [22], obtained by an inelastic electron scattering technique in the energy range 13–100 eV within a total expected uncertainty of ±50%, were added to the cross section for excitation to $a^1\Pi_g$, and also agree with the two sets of recommended data (Graph 15). Hereafter no mention is made about the comparison among plural numbers of data sets except when there are discrepancies.

James et al. [23] measured the cross sections for excitation to ($b^1\Pi_u$; $v = 2$), ($b^1\Pi_u$; $v = 3$), ($b^1\Pi_u$; $v = 4$), ($b^1\Pi_u$; $v = 7$), and ($b^1\Pi_u$; sum over v) (Graphs 17–21) in the energy range 14–400 eV by a crossed-beam technique. The data recommended by Majeed and Strickland [3] in the 13–30 eV range were also used (Graph 21). Ajello et al. [24] measured the cross sections for excitation to ($b'^1\Sigma_u^+$; $v = 12$), ($b'^1\Sigma_u^+$; $v = 14$), ($b'^1\Sigma_u^+$; $v = 15$), ($b'^1\Sigma_u^+$; $v = 16$), ($b'^1\Sigma_u^+$; $v = 17$), and ($b'^1\Sigma_u^+$; sum over v) (Graphs 22–27) in the energy range from 14 or 16 to 400 eV. Data for ($b'^1\Sigma_u^+$; sum over v) in the energy range of 15 eV–1 keV was also taken from the compilation of Majeed and Strickland [3] (Graph 27) as well as the cross section data for excitation to ($c^1\Pi_u$; sum over v) (Graph 28) in the energy range 13 eV–1 keV. Ajello et al. [24] also measured the cross sections for excitation to ($c_4'^1\Sigma_u^+$; $v = 0$), ($c_4'^1\Sigma_u^+$; $v = 4$), and ($c_4'^1\Sigma_u^+$; sum over v) (Graphs 29–31) in the energy range 14–400 eV. The data recommended by Majeed and Strickland [3] in the energy range 14 eV–1 keV were also used (Graph 31).

Zubek [25] measured cross sections for excitation to ($C^3\Pi_u$; $v = 0$), ($C^3\Pi_u$; $v = 1$), ($C^3\Pi_u$; $v = 2$), and ($C^3\Pi_u$; sum over v) (Graphs 32–35) in the energy range from threshold to 17.5 eV with an electron impact spectrometer. Data for ($C^3\Pi_u$; sum over v) have also been taken from the experimental results of Zubek and King [27] at energies of 17.5 and 20 eV, from the compilation by Trajmar et al. [1] in the 15–50 eV range, and from the compilation by Majeed and Strickland [3] in the 12–200 eV range (Graph 35). The cross section for excitation to $E^3\Sigma_g^+$ (Graph 36) was measured by Brunger et al. [26] in the energy range 11.87–12.69 eV with an estimated uncertainty of 40%. Experimental data of Zubek and King [27] at energies of 17.5 and 20 eV and the data from the compilation by Majeed and Strickland [3] in the 15–50 eV range were also included. Data on the cross section of excitation to $a''^1\Sigma_g^+$ (Graph 37) have been taken from the compilation of Trajmar et al. [1] for the energy range 15–50 eV and from the recommendation of Majeed and Strickland [3] for the range 13 eV–1 keV. Campbell et al. [21] also reported the cross sections for excitation to $C^3\Pi_u$, $E^3\Sigma_g^+$, and $a''^1\Sigma_g^+$ (Graphs 35–37) in the energy range from 15 to 50 eV. Their data, obtained from the earlier differential cross section measurements of their group, are in moderate agreement with the results of other authors, except that two data points around the 10 eV peak of the cross section for excitation to $E^3\Sigma_g^+$ show a large discrepancy. We have not used the data of Campbell et al. for determining the parameters of analytic expressions.

In a crossed-beam experiment by the use of an electron impact emission chamber in tandem with two UV spectrometers, Ajello and Shemansky [28] measured the cross section for emission from $a^1\Pi_g \rightarrow X^1\Sigma_g^+$ summed over 120.0–260.0 nm (Graph 38) in the energy range 9.8–200 eV. In the present compilation, their data have been

renormalized by a multiplicative factor of 0.892. This factor has been determined by the use of the new data on the emission cross section of the Lyman α line in the collision of electrons with hydrogen molecules (van der Burgt et al. [29]). The cross section for emission from ($a^1\Pi_g \rightarrow X^1\Sigma_g^+$; $v = 3 \rightarrow 3$) at 149.3 nm (Graph 39) was measured by Ajello [30] in the energy range 10.6–200 eV and by Mumma and Zipf [31] in the 10–17.8 eV range. The cross sections for emission from $b'^1\Sigma_{\mu u}{}^+ \rightarrow X^1\Sigma_g{}^+$ summed over 83.7–96.5 nm (Graph 40) was measured by Ajello et al. [24] in the energy range 14–400 eV.

The cross section for emission from ($C^3\Pi_u \rightarrow B^3\Pi_g$; $v = 0 \rightarrow 0$) at 337.03 nm (Graph 41) was measured by Shemansky and Broadfoot [32] in the energy range from threshold to 50 eV. However, only the data up to 18.5 eV have been used in the present compilation, because those authors noted that the results above 25 or 30 eV appeared to be untrustworthy because of the presence of low energy electrons reflected from the collector of the electron gun. The same cross section was also measured by Imami and Borst [33] in the energy range from threshold to 1 keV, by Zubek [25] in the range up to 17.5 eV, and by Shemansky et al. [34] up to 40 eV. The data in the energy range 15–50 eV compiled by Trajmar et al. [1] were also used for this cross section, as deduced from the excitation cross section, by applying the branching ratio of 0.251 for the emission. The branching ratio has been taken from Shemansky et al. [34]. Shemansky et al. [34] also measured the cross section for emission from ($C^3\Pi_u \rightarrow B^3\Pi_g$; $v = 1 \rightarrow 0$) at 315.80 nm (Graph 42) in the energy range 11.4–40 eV. The cross section for emission from ($C^3\Pi_u \rightarrow B^3\Pi_g$; $v = 0 \rightarrow 2$) at 380.4 nm (Graph 43) was measured by Shaw and Campos [35] in the energy range from threshold to 400 eV. Shemansky and Broadfoot [32] provided experimental data on the cross section for emission from ($B^3\Pi_g \rightarrow A^3\Sigma_u{}^+$; $v = 3 \rightarrow 1$) at 762.6 nm (Graph 44) in the energy range 8.5–28 eV.

The total ionization cross section (Graph 45) was measured by Rapp and Englander-Golden [36] in the energy range from threshold to 1 keV, by Straub et al. [37] in the same energy range within an uncertainty of ±3.5%, and by Tian and Vidal [38] in the range from threshold to 600 eV within an error of about 10%. Straub et al. also measured the cross section for ($N_2{}^+$) production (Graph 46) in the energy range 17 eV–1 keV. Tian and Vidal provided the cross sections for N^+ production (Graph 47), $N^+ + N$ production (Graph 48), and $N^+ + N^+$ production (Graph 49), all in the range from threshold to 600 eV. The cross section for N^+ production (Graph 47) was measured by Straub et al. [37], as well, in the energy range from threshold to 1 keV. There are minor discrepancies between the data of Tian and Vidal and those of Straub et al. Considering the behavior of the results from the threshold energy, the data of the latter authors seem to be more reliable. Therefore, the data of Tian and Vidal at the lowest four energies have not been used in the present formulation of the analytic expression. Straub et al. [37] and Tian and Vidal [38] provided the cross section for N^{2+} production (Graph 50) in the range from threshold to 1 keV. The cross section for $N^{2+} + N$ production (Graph 51) was measured by Tian and Vidal in the range from threshold to 600 eV, and the cross section for $N^+ + N^{2+}$ production (Graph 52), by Tian and Vidal in the 100–450 eV range. There are more sets of old data on partial ionization cross sections of N_2. However, the review article by Tawara and Kato [39] indicates that those data show much scatter, so that we have adopted only the newest data.

The cross section for $N_2^+(X^2\Sigma_g{}^+)$ production (Graph 53) was measured by Abramzon et al. [40] by the use of electron scattering and laser-induced fluorescence techniques in the range from threshold to 180 eV with an uncertainty of 7%. The cross section for the excitation of $[N_2^+(B^2\Sigma_u{}^+ \rightarrow X^2\Sigma_g{}^+; v = 0 \rightarrow 0)]$ at 391.4 nm (Graph 54) was measured by Borst and Zipf [41] in the energy range from threshold to 3 keV. They extrapolated the cross section to 10 keV by fitting the Bethe–Oppenheimer relation to the data in the range 200 eV–3 keV. In the present compilation, both their experimental data and the Bethe–Oppenheimer curve read off at discrete energies from their graph have been adopted. The same cross section was measured by Skubenich and Zapesochnyy [42] in the range from threshold to 400 eV. These authors also measured cross sections for the excitation of $[N_2^+(B^2\Sigma_u{}^+ \rightarrow X^2\Sigma_g{}^+; v = 0 \rightarrow 1)]$ at 427.8 nm (Graph 55), $[N_2^+(B^2\Sigma_u{}^+ \rightarrow X^2\Sigma_g{}^+; v = 0 \rightarrow 2)]$ at 470.9 nm (Graph 56), $[N_2^+(B^2\Sigma_u{}^+ \rightarrow X^2\Sigma_g{}^+; v = 1 \rightarrow 0)]$ at 358.2 nm (Graph 57), $[N_2^+(A^2\Pi_u{}^+ \rightarrow X^2\Sigma_g{}^+; v = 1 \rightarrow 0)]$ at 918.3 nm (Graph 58), $[N_2^+(A^2\Sigma_u{}^+ \rightarrow X^2\Sigma_g{}^+; v = 2 \rightarrow 0)]$ at 785.4 nm (Graph 59), and $[N_2^+(A^2\Pi_u{}^+ \rightarrow X^2\Sigma_g{}^+; v = 3 \rightarrow 0)]$ at 687.4 nm (Graph 60), all in the energy range from threshold to 400 eV.

The cross section for N + N production (Graph 61) has been taken from Cosby's recommendation [43] in the energy range 12–200 eV.

The emission cross section for $N(^4D^0 \rightarrow {}^4P)$ at 868.0 nm (Graph 62) was measured by Aarts and de Heer [44] in the energy range 100–500 eV and by Filippelli et al. [45] in the range 22.4–193 eV. The emission cross section for $N(^4P \rightarrow {}^4S^0)$ at 120.0 nm (Graph 63) was measured by Aarts and de Heer [44] in the energy range 100 eV–5 keV, by Mumma and Zipf [31] in the range 22.5–350 eV, by Forand et al. [46] at an energy of 200 eV, by Ajello et al. [24] at energies 100 and 200 eV, and by James et al. [23] in the 20–200 eV range. The Mumma–Zipf and Aarts–de Heer papers also include the results of measurements of cross sections for emission from $N(^2P \rightarrow {}^2D^0)$ at 149.3 nm (Graph 64) and emission from $N(^2D \rightarrow {}^2D^0)$ at 124.3 nm (Graph 65). The energy range of the Mumma–Zipf data is 100 eV–5 keV and that of the Aarts–de Heer data is from threshold to 350 eV. The emission cross section for $N(^2P \rightarrow {}^2P^0)$ at 174.3 nm (Graph 66) was measured by Ajello [30] in the energy range from threshold to about 200 eV. The emission cross sections for $N(^4P \rightarrow {}^4S^0)$ at 113.4 nm (Graph 67) and $N^+(^3D^0 \rightarrow {}^3P)$ at 108.4 nm (Graph 68) were measured by Aarts and de Heer [44] in

the energy range 60 eV–3 keV and 50–5 keV. Low energy data are deficient for these two cross sections.

1.1.2. The singly ionized nitrogen molecule (N_2^+)

Bahati et al. [47] measured the single ionization cross section (Graph 69) in the energy range from threshold to 2.5 keV. The N^+ production cross section (Graph 70) was measured by Van Zyl and Dunn [48] in the energy range from threshold to about 500 eV.

Peterson et al. [49] measured the $N^+ + N$ production (dissociative excitation or dissociation) cross section (Graph 71) with an ion storage ring in combination with an imaging technique in the energy range from threshold to 54.3 eV. Bahati et al. [47] measured the same cross section by the animated crossed electron-ion beam method in the energy range from threshold to 2.5 keV. The two sets of results show large discrepancies of a factor of about three. Considering that the discrepancies might be partly due to the two experimental methods, Bahati et al. performed many tests to check the possible reason, without reaching a definitive conclusion. At energies below the single-ionization and dissociative-ionization thresholds (about 30 eV), however, one expects the dissociative-excitation cross section to be the same as the N^+ production cross section as observed by Van Zyl and Dunn [48] (Graph 70). The data of Peterson et al. agree with those of Van Zyl and Dunn, while those of Bahati et al. do not. Thus, we adopted the results of Peterson et al., and used only the high-energy trend of the data of Bahati et al. to make an analytic expression.

Bahati et al. also measured the $N^+ + N^+$ production (or dissociative ionization) cross section (Graph 72) from threshold to 2.5 keV. The $N^{2+} + N$ production (asymmetrical dissociative ionization) cross section (Graph 73) was measured by Siari et al. [50] by the animated crossed beams method in the energy range from threshold to approximately 2 keV within the total uncertainty of ±5.5% at the cross section maximum.

The N + N production (or dissociative recombination) cross section (Graph 74) was measured by Peterson et al. [49] in the 0.012–1.18 eV range. Older data obtained by Noren et al. [51] are generally much lower than the results of Peterson et al., and are about five times lower at 0.07 eV. We have not included the data of Noren et al. in the present compilation. Though undulations seen in the data of Peterson et al. are also seen in the data of Noren et al., the present analytic expression neglected this minor behavior.

Crandall et al. [52] measured the cross sections for electron impact excitation (Graph 75) by a crossed-beam technique. The total uncertainty of their results at high confidence is about 18%.

1.2. Analytic expressions

The functional form of the analytic expressions used in the present work are the same as, or similar to, those used in the previous work [10,11]. For cross sections except for ionization, modified forms of equations derived semiempirically by Green and McNeal [53] have been used. For ionization cross sections, use is made of the function with an asymptotic form of $\ln E/E$ (E being the incident electron energy), as proposed by Lotz [54], and with a modified near-threshold form [see Eq. (7) below].

In writing modified Green–McNeal equations, we introduce three different functions of the form:

$$f_1(x; c_1, c_2) = \sigma_0 c_1 (x/E_R)^{c_2}, \tag{i}$$

$$f_2(x; c_1, c_2, c_3, c_4) = f_1(x; c_1, c_2)/[1 + (x/c_3)^{c_2+c_4}], \tag{ii}$$

$$f_3(x; c_1, c_2, c_3, c_4, c_5, c_6) = f_1(x; c_1, c_2)/[1 + (x/c_3)^{c_2+c_4} + (x/c_5)^{c_2+c_6}] \tag{iii}$$

with $\sigma_0 = 1 \times 10^{-16}\,\mathrm{cm}^2$ and $E_R = 1.361 \times 10^{-2}$ keV (one Rydberg). The symbols x and c_i ($i = 1, 2, 3, \ldots, 6$) in Eqs. (i)–(iii) denote dummy parameters. The cross sections recommended in the present paper are expressed by one of the following forms involving the combination of the above functions:

$$\sigma = f_2(E_1; a_1, a_2, a_3, a_4), \tag{1}$$

$$\sigma = f_2(E_1; a_1, a_2, a_3, a_4) + f_2(E_1; a_5, a_6, a_7, a_4), \tag{2}$$

$$\sigma = f_2(E_1; a_1, a_2, a_3, a_4) + f_2(E_1; a_5, a_6, a_7, a_8), \tag{3}$$

$$\sigma = f_2(E_1; a_1, a_2, a_3, a_4) + f_2(E_1; a_5, a_6, a_7, a_8) + f_2(E_1; a_9, a_{10}, a_{11}, a_{12}), \tag{4}$$

$$\sigma = f_3(E_1; a_1, a_2, a_3, a_4, a_5, a_6), \tag{5}$$

$$\sigma = f_3(E_1; a_1, a_2, a_3, a_4, a_5, a_6) + f_2(E_1; a_7, a_8, a_9, a_{10}), \tag{6}$$

$$\sigma = \sigma_0 a_1 \ln(E/E_{\mathrm{th}} + a_2)/[E_{\mathrm{th}} E (1 + a_3/E_1)^{a_4}], \tag{7}$$

where $E_1 = E - E_{\mathrm{th}}$ with E the incident electron energy in keV and E_{th} the threshold energy of reaction in keV. Depending on the formula chosen from Eqs. (1)–(6) above, a_1, a_2, etc., are substituted for c_1, c_2, etc., in f_2 and f_3 given by Eqs. (ii) and (iii).

Tables 1 and 2 (read across two facing pages) give the values of the fitting parameters ($a_1, a_2, \ldots$), which have been determined by least-squares fits to the collected data (in some cases with additional constraints to guarantee reasonable behavior outside the energy range of the available data). The present expressions allow one not only to interpolate but also to extrapolate the data to some extent. This is in contrast to polynomial fits, which frequently show physically unreasonable behavior just outside the energy range of the available data.

The resulting analytic expressions are shown in Graphs together with the compiled data. Normally the present forms fit the data quite well. To show the agreement quantitatively, the root-mean-square and the maximum deviations of the expressions from the data are also given in Tables.

Acknowledgments

We are indebted to Professor Y. Itikawa of the Institute of Space and Astronautical Science for his critical reading of

the manuscript and invaluable comments. Thanks are due to Dr. T. Ozeki of Japan Atomic Energy Research Institute for his encouragement and support of this work. This paper has been prepared as an account of work supported partly by a research contract of Japan Atomic Energy Research Institute with Osaka Nuclear Science Association.

Appendix A. Supplementary material

Supplementary data associated with this article can be found, in the online version, at doi:10.1016/j.adt.2006.02.002.

References

[1] S. Trajmar, D.F. Register, A. Chutjian, Phys. Rep. 97 (1983) 219.
[2] Y. Itikawa, M. Hayashi, A. Ichimura, K. Onda, K. Sakimoto, K. Takayanagi, M. Nakamura, H. Nishimura, T. Takayanagi, J. Phys. Chem. Ref. Data 15 (1986) 985.
[3] T. Majeed, D.J. Strickland, J. Phys. Chem. Ref. Data 26 (1997) 335.
[4] L.J. Kieffer, "Bibliography of Low Energy Electron and Photon Cross Section Data (through December 1974)," NBS Special Publication 426, Natl. Bureau of Standards, 1976.
[5] L.J. Kieffer, J.R. Rumble, E.C. Beaty, "Bibliography of Low Energy Electron and Photon Cross Section Data (January 1975 through December 1977)," NBS Special Publication 426, Suppl. 1, Natl. Bureau of Standards, 1979.
[6] J.W. Gallagher, E.C. Beaty, "Bibliography of Low Energy Electron and Photon Cross Section Data (1978)," Univ. Colorado JILA Information Center Rep. No. 18, 1980.
[7] J.W. Gallagher, E.C. Beaty, "Bibliography of Low Energy Electron and Photon Cross Section Data (1979)," Univ. Colorado JILA Information Center Rep. No. 21, 1981.
[8] Y. Itikawa, "Bibliography on Electron Collisions with Molecules: Rotational and Vibrational Excitations, 1980–2000," Natl. Inst. Fusion Sci. Rep. NIFS-DATA-63, 2001.
[9] M. Hayashi, "Bibliography of Electron and Photon Cross Sections with Atoms and Molecules Published in the 20th Century – Nitrogen Molecule," Natl. Inst. Fusion Sci. Rep. NIFS-DATA-77, 2003.
[10] T. Shirai, T. Tabata, H. Tawara, At. Data Nucl. Data Tables 79 (2001) 143.
[11] T. Shirai, T. Tabata, H. Tawara, Y. Itikawa, At. Data Nucl. Data Tables 80 (2002) 1.
[12] J.C. Nickel, I. Kanik, S. Trajmar, K. Imre, J. Phys. B 25 (1992) 2427.
[13] H. Nishimura, K. Yano, J. Phys. Soc. Jpn. 57 (1988) 1951.
[14] K.R. Hoffman, M.S. Dababneh, Y.-F. Hsieh, W.E. Kauppila, V. Pol, J.H. Smart, T.S. Stein, Phys. Rev. A 25 (1982) 1393.
[15] M.J. Brennan, D.T. Alle, P. Euripides, S.J. Buckman, M.J. Brunger, J. Phys. B 25 (1992) 2669.
[16] G. García, A. Pérez, J. Campos, Phys. Rev. A 38 (1988) 654.
[17] M. Hayashi, "Recommended Values of Transport Cross Sections for Elastic Collision and Total Collision Cross Section for Electrons in Atomic and Molecular Gases," Inst. Plasma Phys. Nagoya Univ. Rep. IPPJ-AM-19, 1981.
[18] X. Shi, T.M. Stephen, P.D. Burrow, J. Phys. B 26 (1993) 121.
[19] K. Onda, J. Phys. Soc. Jpn. 54 (1985) 4544.
[20] C.J. Sweeney, T.W. Shyn, Phys. Rev. A 56 (1997) 1384.
[21] L. Campbell, M.J. Brunger, A.M. Nolan, L.J. Kelly, A.B. Wedding, J. Harrison, P.J.O. Teubner, D.C. Cartwright, B. McLaughlin, J. Phys. B 34 (2001) 1185.
[22] T.G. Finn, J.P. Doering, J. Chem. Phys. 64 (1976) 4490.
[23] G.K. James, J.M. Ajello, B. Franklin, D.E. Shemansky, J. Phys. B 23 (1990) 2055.
[24] J.M. Ajello, G.K. James, B.O. Franklin, D.E. Shemansky, Phys. Rev. A 40 (1989) 3524.
[25] M. Zubek, J. Phys. B 27 (1994) 573.
[26] M.J. Brunger, P.J.O. Teubner, S.J. Buckman, Phys. Rev. A 37 (1988) 3570.
[27] M. Zubek, G.C. King, J. Phys. B 27 (1994) 2613.
[28] J.M. Ajello, D.E. Shemansky, J. Geophys. Res. 90 (1985) 9845.
[29] P.J.M. van der Burgt, W.B. Westerveld, J.S. Risley, J. Phys. Chem. Ref. Data 18 (1989) 1757.
[30] J.M. Ajello, J. Chem. Phys. 53 (1970) 1156.
[31] M.J. Mumma, E.C. Zipf, J. Chem. Phys. 55 (1971) 5582.
[32] D.E. Shemansky, A.L. Broadfoot, J. Quant. Spectrosc. Radiat. Transf. 11 (1971) 1401.
[33] M. Imami, W.L. Borst, J. Chem. Phys. 61 (1974) 1115.
[34] D.E. Shemansky, J.M. Ajello, I. Kanik, Astrophys. J. 452 (1995) 472.
[35] M. Shaw, J. Campos, J. Quant. Spectrosc. Radiat. Transf. 30 (1983) 73.
[36] D. Rapp, P. Englander-Golden, J. Chem, Physica 43 (1965) 1464.
[37] H.C. Straub, P. Renault, B.G. Lindsay, K.A. Smith, R.F. Stebbings, Phys. Rev. A 54 (1996) 2146.
[38] C. Tian, C.R. Vidal, J. Phys. B 31 (1998) 5369.
[39] H. Tawara, T. Kato, At. Data Nucl. Data Tables 36 (1987) 167.
[40] N. Abramzon, R.B. Siegel, K. Becker, J. Phys. B 32 (1999) L247.
[41] W.L. Borst, E.C. Zipf, Phys. Rev. A 1 (1970) 834.
[42] V.V. Skubenich, I.P. Zapesochnyy, Geomag. Aeron. 21 (1981) 355.
[43] P.C. Cosby, J. Chem. Phys. 98 (1993) 9544.
[44] J.F.M. Aarts, F.J. de Heer, Physica 52 (1971) 45.
[45] A.R. Filippelli, F.A. Sharpton, C.C. Lin, R.E. Murphy, J. Chem. Phys. 76 (1982) 3597.
[46] J.L. Forand, S. Wang, J.W. Woolsey, J.W. McConkey, Can. J. Phys. 66 (1988) 349.
[47] E.M. Bahati, J.J. Jureta, D.S. Belic, H. Cherkani-Hassani, M.O. Abdellahi, P. Defrance, J. Phys. B 34 (2001) 2963.
[48] B. Van Zyl, G.H. Dunn, Phys. Rev. 163 (1967) 43.
[49] J.R. Peterson, A. Le Padellec, H. Danared, G.H. Dunn, M. Larsson, A. Larson, R. Peverall, C. Strömholm, S. Rosén, M. af Ugglas, W.J. van der Zande, J. Chem. Phys. 108 (1998) 1978.
[50] A. Siari, D.S. Belic, P. Defrance, S. Rachafi, J. Phys. B 32 (1999) 587.
[51] C. Noren, F.B. Yousif, J.B.A. Mitchell, J. Chem. Soc. Faraday Trans. 85 (1989) 1697.
[52] D.H. Crandall, W.E. Kauppila, R.A. Phaneuf, P.O. Taylor, G.H. Dunn, Phys. Rev. A 9 (1974) 2545.
[53] A.E.S. Green, R.J. McNeal, J. Geophys. Res. 76 (1971) 133.
[54] W. Lotz, Z. Phys. 206 (1967) 205.

Explanation of Tables

Table 1. Energy ranges of data, fitting errors, and parameters of the analytic expressions for nitrogen molecules, N_2

No.	Number label identifying a particular reaction process in the same sequence as in the Graphs
Process	The relevant reaction process
E_{min}	Minimum energy (in keV) of experimental data
E_{max}	Maximum energy (in keV) of experimental data
δ_{rms}	Root-mean-square relative deviation (in %) of the analytic expression from the data
δ_{max}	Maximum relative deviation (in %) of the analytic expression from the data
$E_{\delta_{max}}$	Energy (in keV) at which the relative deviation takes on the value δ_{max}
Eq.	The identifying number of the equation to be used for deriving the recommended cross sections
n	Number of applicable fit parameters
E_{th}	Threshold energy of the reaction (in keV)
$a_j (j = 1, 2, \ldots, 12)$	Fit parameters

The notation $1.23-1$ means 1.23×10^{-1}.

Table 2. Energy ranges of data, fitting errors, and parameters of the analytic expressions for singly ionized nitrogen molecules, (N_2^+)

Same as for Table 1.

Explanation of Graphs

Graphs 1–75. Cross section vs. electron energy

Graphs are numbered in the same sequence as in Tables 1 and 2

Ordinate	Cross section in cm^2
Abscissa	Electron energy in eV in the laboratory system
Solid line	Recommended data from the analytic formula of the present work
Symbols	Experimental data from sources as explained in the legends

Table 1
Energy ranges of data, fitting errors, and parameters of the analytic expressions for nitrogen molecules, N_2. See page 381 for Explanation of Tables

No.	Process	E_{min}	E_{max}	δ_{rms}	δ_{max}	$E_{\delta_{max}}$
1	Total scattering	5.14−5	5.00+0	4.7+0	1.5+1	1.50−3
2	Elastic scattering	5.14−5	5.22+0	3.6+0	9.1+0	1.50−3
3	Momentum transfer	1.05−5	3.44+0	6.1+0	1.5+1	8.07−3
4	Rotational excitation J=0 → 2	2.96−5	2.94−3	6.0+0	1.1+1	4.05−4
5	Vibrational excitation $v = 0 \rightarrow 1$	1.05−3	4.85−2	2.6+1	6.6+1	2.01−3
6	Vibrational excitation $v = 0 \rightarrow 2$	...	...	...	...	...
7	Vibrational excitation $v = 0 \rightarrow 3$	...	...	...	...	...
8	Vibrational excitation $v = 0 \rightarrow 4$	...	...	...	...	...
9	Total vibrational excitation	1.30−3	6.00−3	3.5+1	5.3+1	4.00−3
10	Excitation to $A^3\Sigma_u^+$	6.50−3	2.00−1	1.9+1	4.8+1	5.00−2
11	Excitation to $B^3\Pi_g$	7.60−3	2.00−1	9.1+0	2.1+1	1.50−1
12	Excitation to $W^3\Delta_u$	8.00−3	2.00−1	1.7+1	5.1+1	1.00−2
13	Excitation to $B'^3\Sigma_u^-$	9.00−3	2.00−1	1.3+1	3.0+1	2.00−2
14	Excitation to $a'^1\Sigma_u^-$	1.10−2	1.00+0	9.4+0	2.2+1	1.70−2
15	Excitation to $a^1\Pi_g$	1.00−2	1.00+0	1.3+1	3.5+1	1.00−2
16	Excitation to $w^1\Delta_u$	9.00−3	2.00−1	1.3+1	3.6+1	2.00−2
17	Excitation to $b^1\Pi_u$; $v = 2$	1.40−2	4.00−1	0.6+0	1.1+0	6.00−2
18	Excitation to $b^1\Pi_u$; $v = 3$	1.40−2	4.00−1	0.6+0	0.9+0	6.00−2
19	Excitation to $b^1\Pi_u$; $v = 4$	1.40−2	4.00−1	0.7+0	1.2+0	1.60−2
20	Excitation to $b^1\Pi_u$; $v = 7$	1.40−2	4.00−1	0.7+0	1.1+0	6.00−2
21	Excitation to $b^1\Pi_u$	1.30−2	4.00−1	1.1+1	3.2+1	1.40−2
22	Excitation to $b'^1\Sigma_u^+$; $v = 12$	1.40−2	4.00−1	0.8+0	1.5+0	2.00−1
23	Excitation to $b'^1\Sigma_u^+$; $v = 14$	1.60−2	4.00−1	0.4+0	0.8+0	1.00−1
24	Excitation to $b'^1\Sigma_u^+$; $v = 15$	1.60−2	4.00−1	0.4+0	0.7+0	1.00−1
25	Excitation to $b'^1\Sigma_u^+$; $v = 16$	1.60−2	4.00−1	0.5+0	1.1+0	1.00−1
26	Excitation to $b'^1\Sigma_u^+$; $v = 17$	1.60−2	4.00−1	0.3+0	0.8+0	1.00−1
27	Excitation to $b'^1\Sigma_u^+$	1.40−2	1.00+0	1.2+1	3.5+1	1.50−2
28	Excitation to $c^1\Pi_u$	1.30−2	1.00+0	3.4+0	7.8+0	5.00−2
29	Excitation to $c_4'^1\Sigma_u^+$; $v = 0$	1.40−2	4.00−1	0.1+0	0.2+0	1.80−2
30	Excitation to $c_4'^1\Sigma_u^+$; $v = 4$	1.60−2	4.00−1	0.1+0	0.2+0	6.00−2
31	Excitation to $c_4'^1\Sigma_u^+$	1.40−2	1.00+0	1.8+0	4.1+0	1.60−2
32	Excitation to $C^3\Pi_u$; $v = 0$	1.13−2	1.75−2	0.6+0	1.3+0	1.38−2
33	Excitation to $C^3\Pi_u$; $v = 1$	1.13−2	1.75−2	4.2+0	1.5+1	1.15−2
34	Excitation to $C^3\Pi_u$; $v = 2$	1.18−2	1.70−2	2.2+0	4.9+0	1.20−2
35	Excitation to $C^3\Pi_u$	1.13−2	2.00−1	9.5+0	3.4+1	1.30−2
36	Excitation to $E^3\Sigma_g^+$	1.19−2	5.00−2	1.1+1	2.9+1	1.70−2
37	Excitation to $a''^1\Sigma_g^+$	1.30−2	1.00+0	1.1+1	3.3+1	3.00−2
38	Emission from $a^1\Pi_g \rightarrow X^1\Sigma_g^+$ over 120.0–260.0 nm	1.00−2	2.00−1	2.6+0	6.5+0	1.20−2
39	Emission from $a^1\Pi_g \rightarrow X^1\Sigma_g^+$; $v = 3 \rightarrow 3$; at 149.3 nm	1.00−2	2.00−1	4.7+0	1.0+1	1.25−2
40	Emission from $b'^1\Sigma_u^+ \rightarrow X^1\Sigma_g^+$ over 85.7–94.5 nm	1.40−2	4.00−1	1.4+0	2.2+0	1.80−2
41	Emission from $C^3\Pi_u \rightarrow B^3\Pi_g$; $v = 0 \rightarrow 0$ at 337.03 nm	1.11−2	3.00−1	2.0+1	8.9+1	1.15−2
42	Emission from $C^3\Pi_u \rightarrow B^3\Pi_g$; $v = 1 \rightarrow 0$ at 315.80 nm	1.14−2	4.02−2	5.3+0	1.5+1	1.16−2
43	Emission from $C^3\Pi_u \rightarrow B^3\Pi_g$; $v = 0 \rightarrow 2$ at 380.4 nm	1.18−2	4.00−1	3.2+0	5.1+0	3.82−2
44	Emission from $B^3\Pi_g \rightarrow A^3\Sigma_u^+$; $v = 3 \rightarrow 1$ at 762.6 nm	8.50−3	2.78−2	3.6+0	7.5+0	1.07−2
45	Total ionization	1.60−2	1.00+0	1.2+1	8.4+1	1.70−2
46	(N_2^+) Production	1.70−2	1.00+0	4.2+0	1.3+1	2.00−2

Table 1 (*continued*)
Energy ranges of data, fitting errors, and parameters of the analytic expressions for nitrogen molecules, N_2. See page 381 for Explanation of Tables

No.	Eq.	n	E_{th}	a_1	a_2	a_3	a_4	a_5	a_6
				a_7	a_8	a_9	a_{10}	a_{11}	a_{12}
1	6	10	0.00+0	6.130+4	1.530+0	3.110−5	−1.540−1	9.310−4	8.770−1
				9.170+7	8.320+0	2.362−3	6.050+0		
2	6	10	0.00+0	1.440+4	1.284+0	3.190−5	−1.550−1	9.000−4	8.600−1
				9.140+5	6.180+0	2.437−3	5.980+0		
3	6	10	0.00+0	1.370+2	5.820−1	4.010−4	1.280−1	9.290−3	1.545+0
				1.960+7	7.820+0	2.370−3	5.870+0		
4	2	7	1.50−6	1.120+8	3.146+0	4.180−5	2.670−1	4.370+7	8.980+0
				2.071−3					
5	4	12	2.90−4	1.83+10	1.000+1	9.410−4	4.200−1	1.240+9	1.000+1
				2.087−3	7.980+0	1.370−2	9.200+0	1.940−2	6.900+0
6	...	...							
7	...	...							
8	...	...							
9	4	12	2.90−4	1.730−2	5.510−1	3.510−2	2.320+0	9.070+9	1.000+1
				1.970−3	6.390+0	1.530−2	7.970+0	2.020−2	9.150+0
10	1	4	6.17−3	3.970−1	9.330−1	1.330−2	2.503+0		
11	5	6	7.35−3	6.820+0	1.774+0	3.310−3	9.150−1	1.300−2	3.650+0
12	5	6	7.36−3	9.140−1	1.310+0	9.900−3	2.230+0	3.100−2	4.500+0
13	3	8	8.16−3	7.500−1	1.970+0	6.700−3	3.030+0	2.120−2	1.500−1
				5.780−2	3.390+0				
14	3	8	8.40−3	6.090−1	1.550+0	6.230−3	2.630+0	8.260−3	2.100+0
				2.720−2	1.061+0				
15	1	4	8.55−3	2.560+0	2.040+0	6.690−3	9.300−1		
16	5	6	8.89−3	1.220+0	1.361+0	3.770−3	1.430+0	2.130−2	4.510+0
17	1	4	1.27−2	3.702−2	9.461−1	1.618−2	6.094−1		
18	1	4	1.28−2	6.795−2	9.396−1	1.646−2	6.126−1		
19	1	4	1.28−2	1.097−1	9.774−1	1.599−2	6.037−1		
20	1	4	1.32−2	2.774−2	9.439−1	1.689−2	6.113−1		
21	5	6	1.25−2	8.910+4	6.020+0	9.880−4	−1.290+0	2.070−3	5.750−1
22	5	6	1.39−2	2.464−2	1.612+0	1.118−2	−2.000−2	3.120−2	8.700−1
23	5	6	1.41−2	4.160−2	1.702+0	9.080−3	−2.930−1	1.970−2	6.660−1
24	5	6	1.42−2	5.340−2	1.690+0	9.120−3	−2.980−1	1.970−2	6.600−1
25	5	6	1.42−2	7.120−2	1.761+0	8.430−3	−3.720−1	1.780−2	6.290−1
26	5	6	1.43−2	3.560−2	1.725+0	9.020−3	−2.990−1	1.980−2	6.690−1
27	5	6	1.29−2	2.280+0	3.800+0	5.030−3	−7.700−1	9.800−3	5.900−1
28	5	6	1.21−2	9.020+4	7.330+0	1.700−3	−1.230+0	2.970−3	5.720−1
29	5	6	1.29−2	2.257−1	2.052+0	5.650−3	−7.270−1	1.694−2	5.930−1
30	5	6	1.40−2	2.365−2	1.923+0	7.747−3	−6.290−1	2.119−2	6.169−1
31	5	6	1.29−2	2.170−1	2.041+0	7.830−3	−5.550−1	2.230−2	7.020−1
32	3	8	1.10−2	9.740+2	4.898+0	2.617−3	2.140+0	2.390−1	8.570−1
				8.570−3	1.310+0				
33	3	8	1.12−2	3.100+4	7.150+0	2.490−3	8.000−1	1.050−1	7.830−1
				3.640−3	9.500+0				
34	3	8	1.15−2	7.390+2	5.630+0	2.742−3	1.390+0	1.090−2	4.740−1
				3.770−3	3.400+1				
35	3	8	1.10−2	6.820+2	4.750+0	3.060−3	3.620+0	1.000+0	1.212+0
				6.170−3	1.529+0				
36	4	12	1.19−2	1.750−2	−3.280−1	3.730−4	9.550+0	7.190+7	6.750+0
				6.290−4	4.350+0	1.540−2	1.210+0	1.230−2	2.050+0
37	3	8	1.23−2	8.880−1	1.860+0	3.560−3	3.770+0	1.140+2	8.420+0
				5.680−3	8.930−1				
38	1	4	8.55−3	1.750+0	1.937+0	6.790−3	8.610−1		
39	1	4	8.30−3	2.540−2	9.090−1	3.740−3	3.650−1		
40	5	6	1.29−2	1.320+0	3.995+0	3.080−3	−1.128+0	6.600−3	4.740−1
41	3	8	1.10−2	2.260+1	3.090+0	2.900−3	1.587+0	1.070−2	3.900−1
				2.540−2	2.730+0				
42	3	8	1.13−2	1.440+2	4.440+0	2.580−3	1.820+0	2.540−2	5.520−1
				1.220−2	1.580+0				
43	3	8	1.10−2	9.350−2	2.000+0	6.000−3	3.670+0	2.050−1	8.930−1
				2.570−3	7.490−1				
44	6	10	7.97−3	2.04+12	1.000+1	5.817−4	−6.100−1	1.340−3	5.600+0
				4.360+2	1.000+1	6.020−3	1.010+0		
45	7	4	1.56−2	3.460−3	7.000−2	5.750−2	1.023+0		
46	7	4	1.56−2	2.639−3	0.000+0	4.690−2	9.750−1		

(*continued on next page*)

Table 1 (*continued*)
Energy ranges of data, fitting errors, and parameters of the analytic expressions for nitrogen molecules, N_2. See page 381 for Explanation of Tables

No.	Process	E_{min}	E_{max}	δ_{rms}	δ_{max}	$E_{\delta_{max}}$
47	N^+ production	3.00−2	1.00+0	2.9+0	1.0+1	4.50−2
48	$N^+ + N$ production	2.50−2	6.00−1	2.9+0	5.0+0	6.00−1
49	$N^+ + N^+$ production	4.50−2	6.00−1	2.6+0	8.0+0	5.00−2
50	N^{2+} Production	7.00−2	1.00+0	1.5+1	7.7+1	7.00−2
51	$N^{2+} + N$ Production	7.00−2	5.50−1	3.5+0	7.6+0	1.75−1
52	$N^+ + N^{2+}$ Production	1.00−1	4.50−1	0.7+0	1.7+0	4.00−1
53	$N_2^+(X^2\Sigma_g^+)$ production	3.00−2	1.80−1	4.9+0	1.0+1	5.50−2
54	Excitation to $N_2^+(B^2\Sigma_u^+ \rightarrow X^2\Sigma_g^+;\ v=0\rightarrow 0)$ at 391.4 nm	1.90−2	1.00+1	6.2+0	3.5+1	2.05−2
55	Excitation to $N_2^+(B^2\Sigma_u^+ \rightarrow X^2\Sigma_g^+;\ v=0\rightarrow 1)$ at 427.8 nm	2.05−2	3.99−1	3.9+0	9.6+0	3.16−2
56	Excitation to $N_2^+(B^2\Sigma_u^+ \rightarrow X^2\Sigma_g^+;\ v=0\rightarrow 2)$ at 470.9 nm	2.05−2	3.99−1	0.8+0	1.4+0	2.23−1
57	Excitation to $N_2^+(B^2\Sigma_u^+ \rightarrow X^2\Sigma_g^+;\ v=1\rightarrow 0)$ at 358.2 nm	2.92−2	4.00−1	1.7+0	3.5+0	3.01−1
58	Excitation to $N_2^+(A^2\Pi_u^+ \rightarrow X^2\Sigma_g^+;\ v=1\rightarrow 0)$ at 918.3 nm	1.70−2	3.99−1	0.7+0	1.6+0	7.14−2
59	Excitation to $N_2^+(A^2\Pi_u^+ \rightarrow X^2\Sigma_g^+;\ v=2\rightarrow 0)$ at 785.4 nm	1.73−2	3.99−1	0.7+0	1.7+0	1.92−1
60	Excitation to $N_2^+(A^2\Pi_u^+ \rightarrow X^2\Sigma_g^+;\ v=3\rightarrow 0)$ at 687.4 nm	1.75−2	3.97−1	1.5+0	2.7+0	3.97−1
61	N + N production	1.20−2	2.00−1	1.2+1	3.2+1	1.40−2
62	Emission from $N(^4D^0 \rightarrow {}^4P)$ at 868.0 nm	2.24−2	5.00−1	1.8+0	6.6+0	1.00−1
63	Emission from $N(^4P \rightarrow {}^4S^0)$ at 120.0 nm	2.02−2	5.00+0	8.6+0	3.9+1	2.25−2
64	Emission from $N(^2P \rightarrow {}^2D^0)$ at 149.3 nm	2.05−2	5.00+0	2.4+0	4.9+0	2.75−2
65	Emission from $N(^2D \rightarrow {}^2D^0)$ at 124.3 nm	2.25−2	5.00+0	3.8+0	9.3+0	4.00+0
66	Emission from $N(^2P \rightarrow {}^2P^0)$ at 174.3 nm	2.17−2	1.98−1	4.9+0	1.2+1	2.21−2
67	Emission from $N(^4P \rightarrow {}^4S^0)$ at 113.4 nm	6.00−2	3.00+0	3.5+0	1.0+1	8.00−1
68	Emission from $N^+(^3D^0 \rightarrow {}^3P)$ at 108.4 nm	5.00−2	5.00+0	2.4+0	4.9+0	4.00−1

Table 1 (*continued*)
Energy ranges of data, fitting errors, and parameters of the analytic expressions for nitrogen molecules, N_2. See page 381 for Explanation of Tables

No.	Eq.	n	E_{th}	a_1	a_2	a_3	a_4	a_5	a_6
				a_7	a_8	a_9	a_{10}	a_{11}	a_{12}
47	7	4	2.43–2	5.060−4	4.460+0	6.390−2	1.856+0		
48	7	4	1.80−2	5.060−4	2.640−1	3.540−2	2.362+0		
49	7	4	3.40−2	2.730−6	3.350+2	7.460−2	2.116+0		
50	5	6	5.39−2	1.030−4	5.500+0	2.380−2	−1.730+0	4.470−2	8.700−1
51	5	6	5.39−2	6.400−4	2.140+0	6.350−2	3.500−1	2.000−1	2.400+0
52	5	6	6.85−2	1.496−4	2.583+0	5.762−2	−1.187+0	8.596–2	1.096+0
53	1	4	1.56−2	3.310−1	1.440+0	3.570−2	4.000−1		
54	5	6	1.88−2	9.260−2	1.030+0	5.250−2	2.700−1	1.050−1	9.100−1
55	1	4	1.88−2	2.760−2	5.880−1	1.330−1	8.700−1		
56	5	6	1.88−2	1.510−1	2.720+0	2.360−3	−8.520−1	9.840−3	5.640−1
57	1	4	1.90−2	6.260−3	7.110−1	8.770−2	6.490−1		
58	5	6	1.69−2	6.920−2	8.104−1	7.770−2	6.610−1	3.360−1	3.880+0
59	5	6	1.72−2	5.670−2	1.236+0	1.200−2	−2.850−1	6.070−2	1.160+0
60	1	4	1.74−2	6.560−3	7.617−1	9.230−2	8.280−1		
61	5	6	9.76−3	1.870+0	3.030+0	1.230−2	4.700−2	3.500−2	1.100+0
62	3	8	2.15−2	1.460−2	1.009+0	7.840−3	2.930+0	5.350−3	1.610+0
				3.670−2	5.360−1				
63	3	8	2.01−2	2.830−6	8.200+0	3.970−2	7.800−1	1.093−2	9.800−1
				7.800−2	7.300−1				
64	6	10	2.04−2	5.290−3	1.690+0	4.600−2	5.300−2	5.400−2	8.870−1
				3.910−3	2.410−1	1.281−2	8.300+0		
65	6	10	2.21−2	1.620+2	1.000+1	4.010−3	−1.167+0	6.620−3	8.694−1
				8.380−4	2.440−1	1.420−2	1.000+1		
66	6	10	2.04−2	6.870−4	1.000+1	1.757−2	−8.000−1	2.320−2	8.000−1
				1.680−2	7.700−1	9.400−3	8.000−1		
67	1	4	2.01−2	7.270−3	7.000−1	6.630−2	8.520−1		
68	1	4	3.57−2	2.298−2	3.930−1	1.200−1	9.540−1		

Table 2
Energy ranges of data, fitting errors, and parameters of the analytic expressions for singly ionized nitrogen molecules, (N_2^+). See page 381 for Explanation of Tables

No.	Process	E_{min}	E_{max}	δ_{rms}	δ_{max}	$E_{\delta_{max}}$
69	Single ionization	2.90−2	2.50+0	6.2+0	1.4+1	3.30−2
70	N^+ production	1.00−2	4.99−1	2.9+0	8.6+0	1.92−2
71	$N^+ + N$ production	9.11−3	5.43−2	9.4+0	2.0+1	9.95−3
72	$N^+ + N^+$ production	3.30−2	2.50+0	8.4+0	2.3+1	3.90−2
73	$N^{2+} + N$ production	4.42−2	2.00+0	1.1+1	4.2+1	4.52−2
74	$N + N$ production	1.23−6	1.18−3	9.0+0	2.0+1	6.18−5
75	Excitation to ($B^2\Sigma_u^+$; $v = 0$)	3.40−3	9.10−2	4.3+0	8.60+0	9.10−2

Table 2 (*continued*)
Energy ranges of data, fitting errors, and parameters of the analytic expressions for singly ionized nitrogen molecules, (N_2^+). See page 381 for Explanation of Tables

No.	Eq.	n	E_{th}	a_1	a_2	a_3	a_4	a_5	a_6
				a_7	a_8	a_9	a_{10}	a_{11}	a_{12}
69	7	4	2.79−2	4.080−5	1.700+2	2.820−1	1.026+0		
70	5	6	8.71−3	1.990+1	1.560+0	2.410−3	−4.210−1	2.000−2	8.750−1
71	1	4	8.40−3	3.280+0	7.330−1	1.840−2	5.760−1		
72	1	4	3.12−2	9.230−2	1.099+0	6.530−2	7.670−1		
73	5	6	3.63−2	3.390−3	6.300+0	1.220−2	−1.310+0	2.050−2	7.680−1
74	1	4	0.00+0	4.000+0	−6.600−1	1.300−4	1.260+0		
75	1	4	3.17−3	5.540+0	1.360−1	3.100−3	8.060−1		

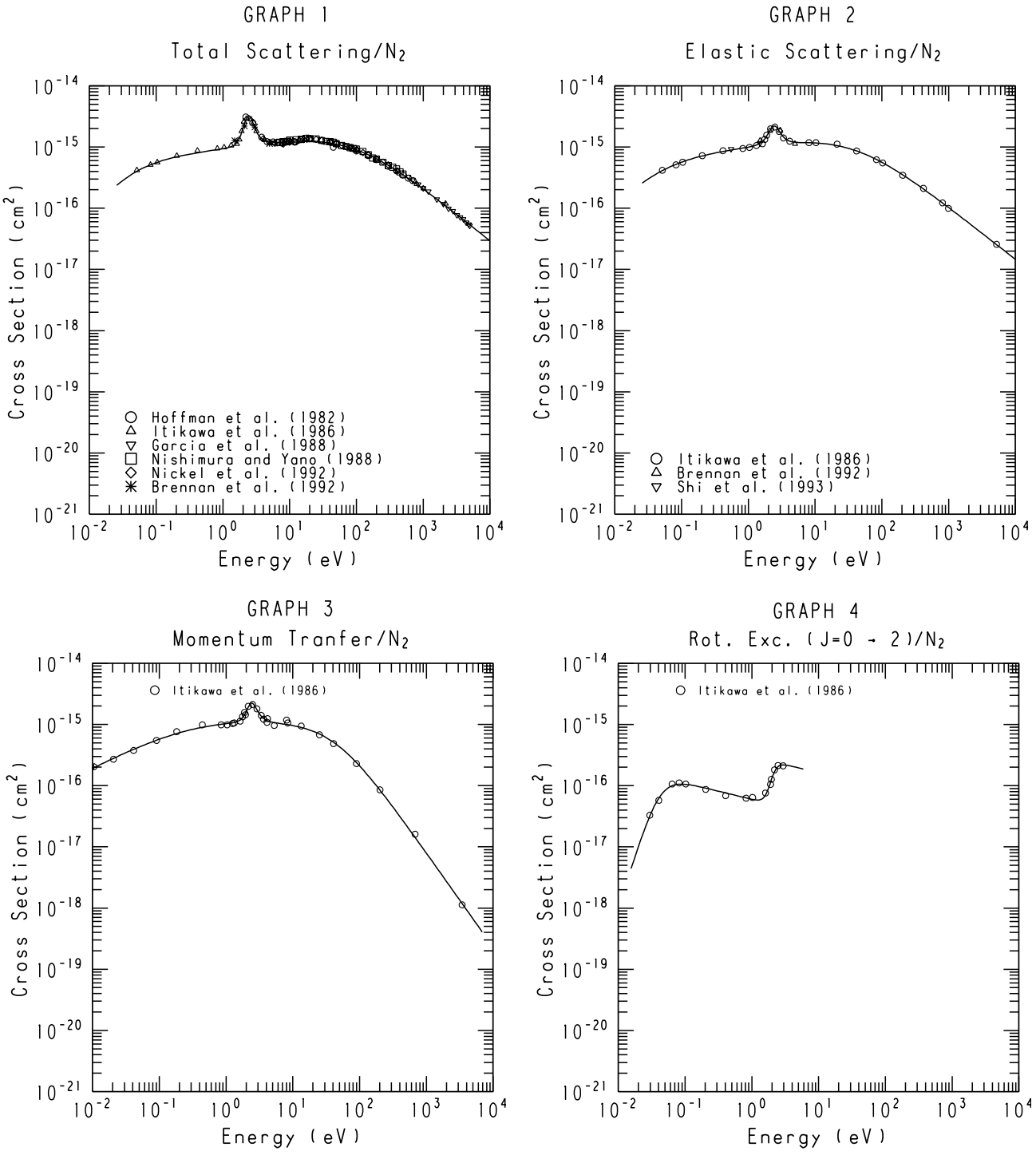

Graphs 1–75. Cross section vs. electron energy.

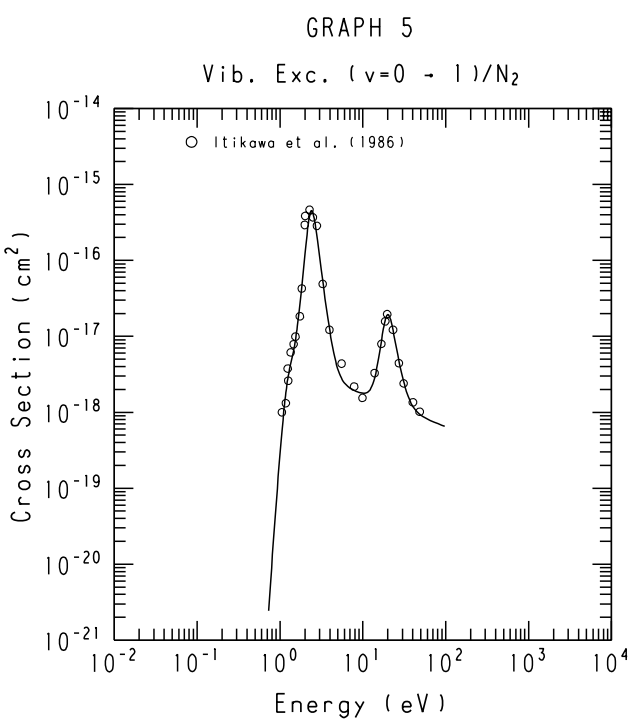

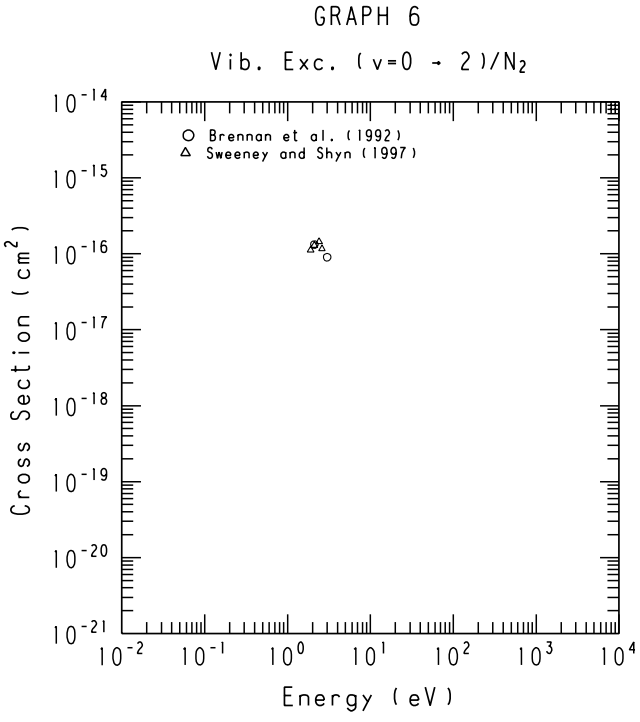

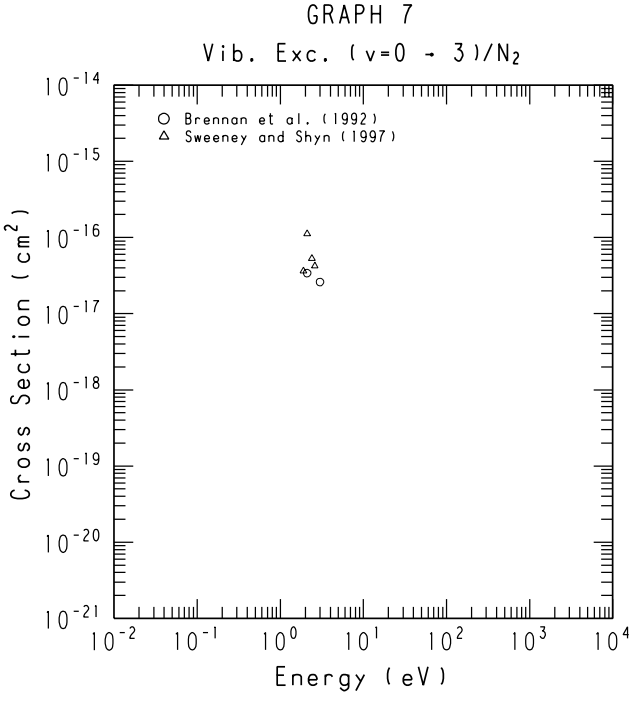

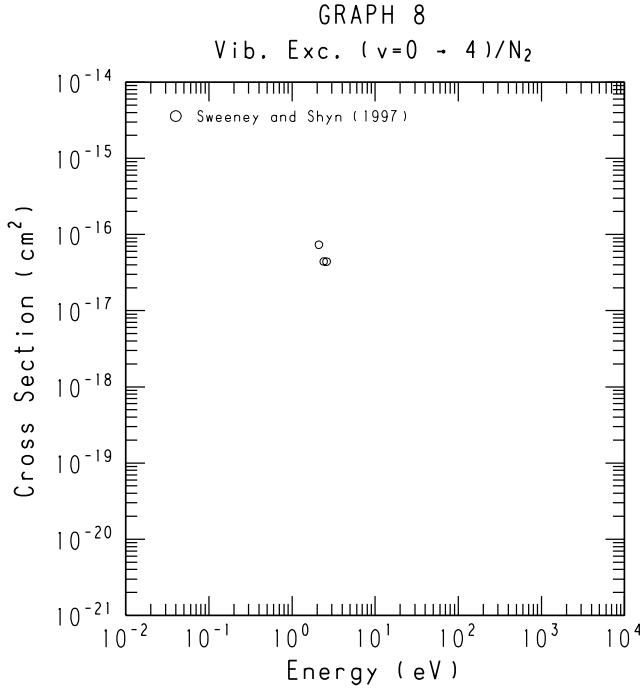

Graphs 1–75. (*continued*)

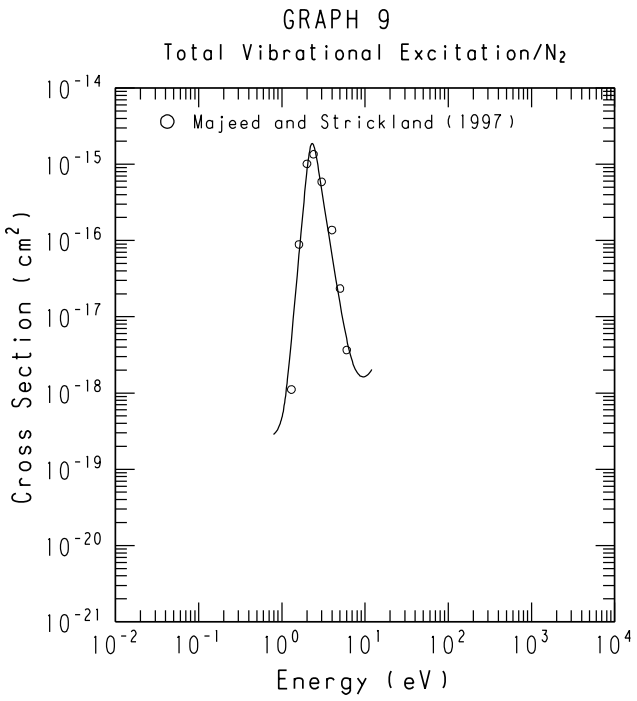

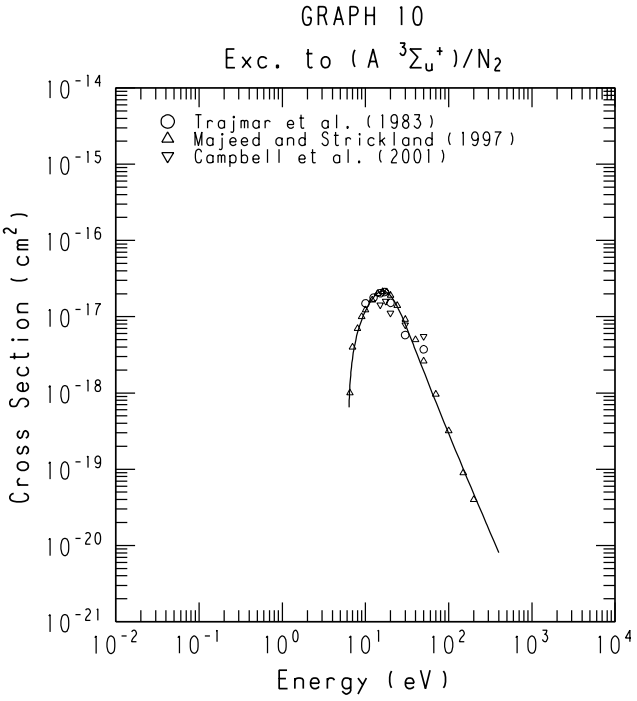

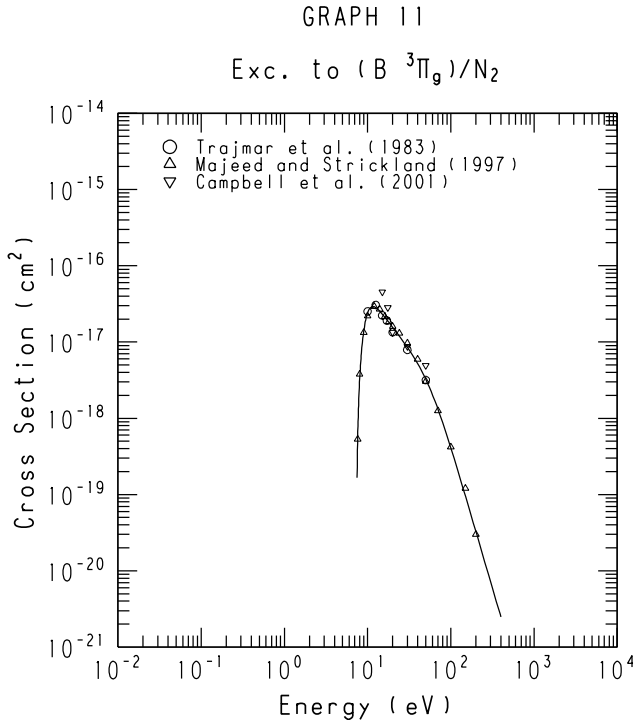

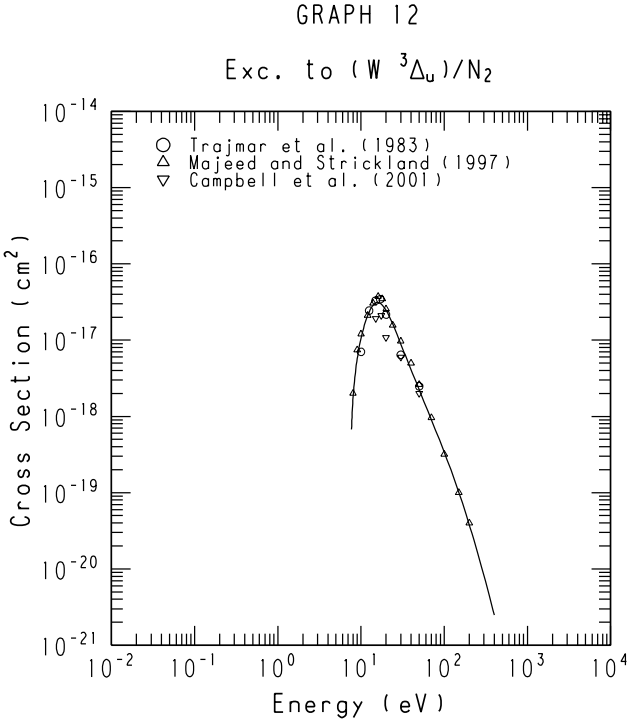

Graphs 1–75. (*continued*)

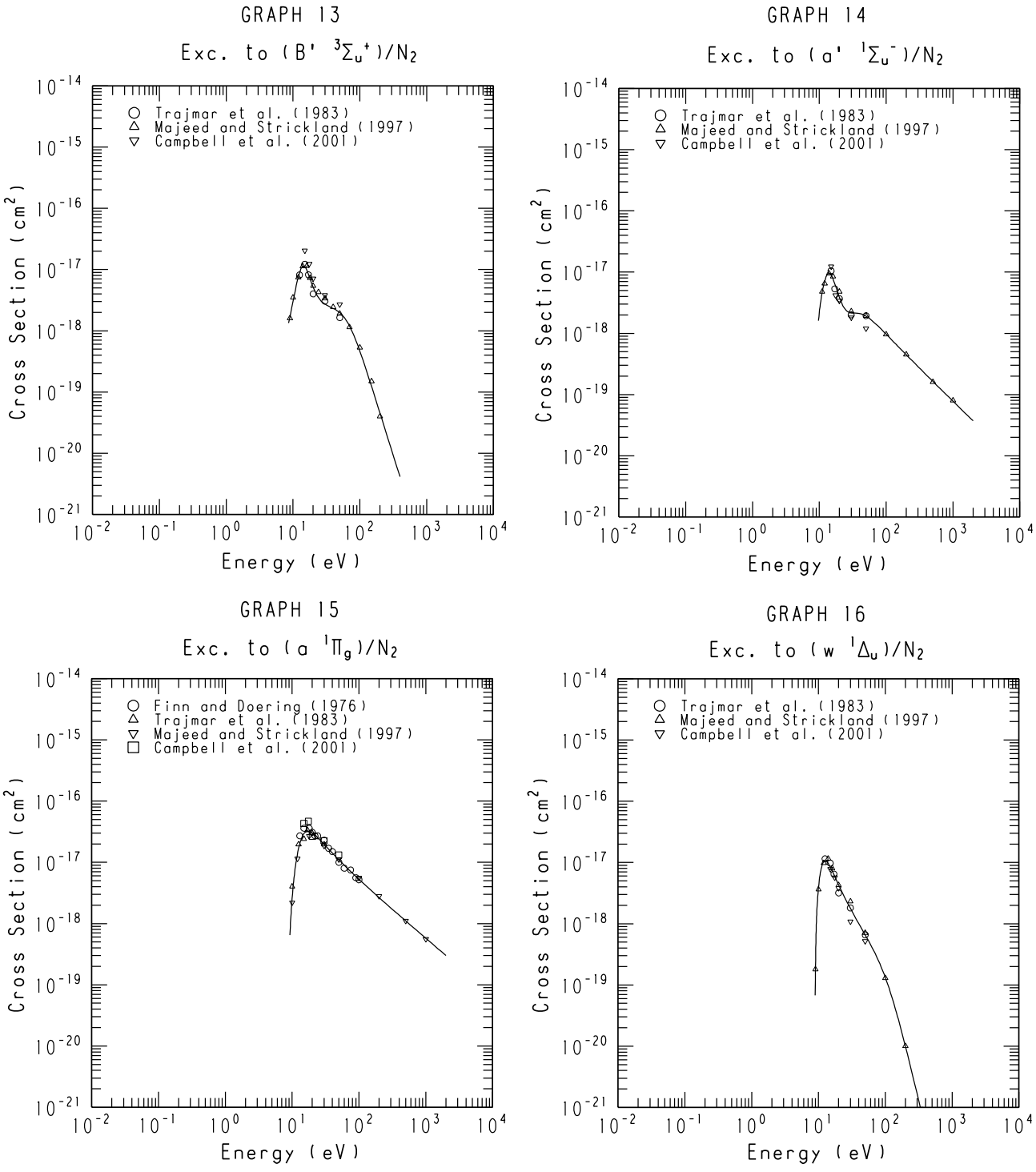

Graphs 1–75. (*continued*)

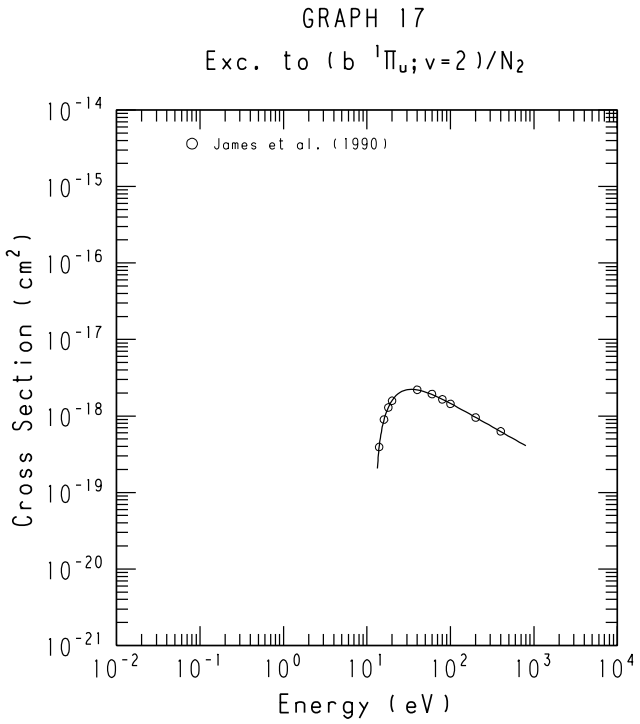

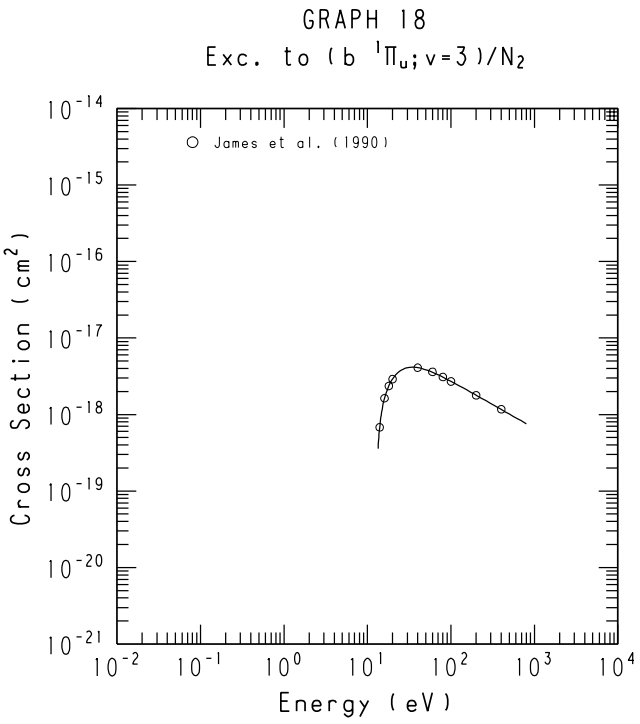

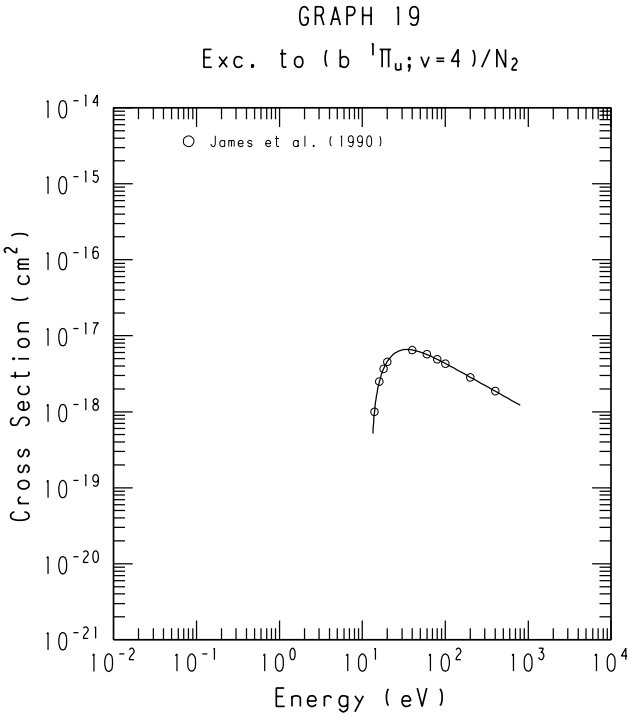

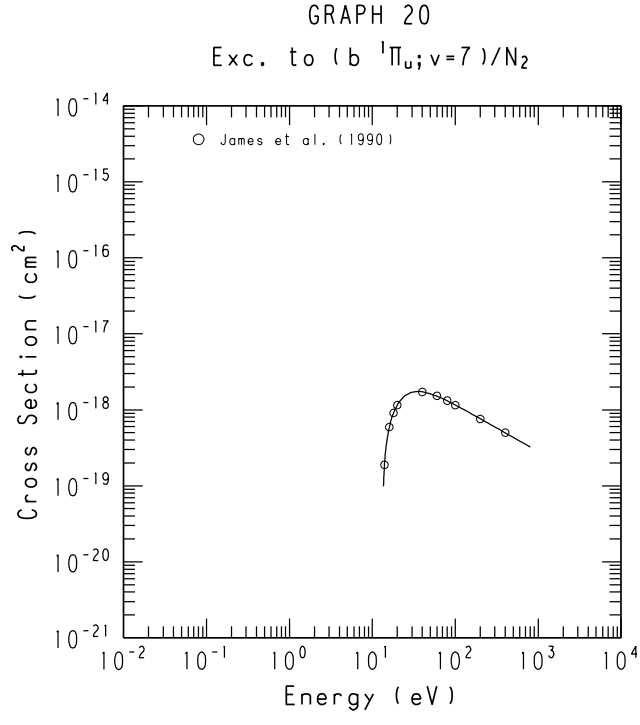

Graphs 1–75. (*continued*)

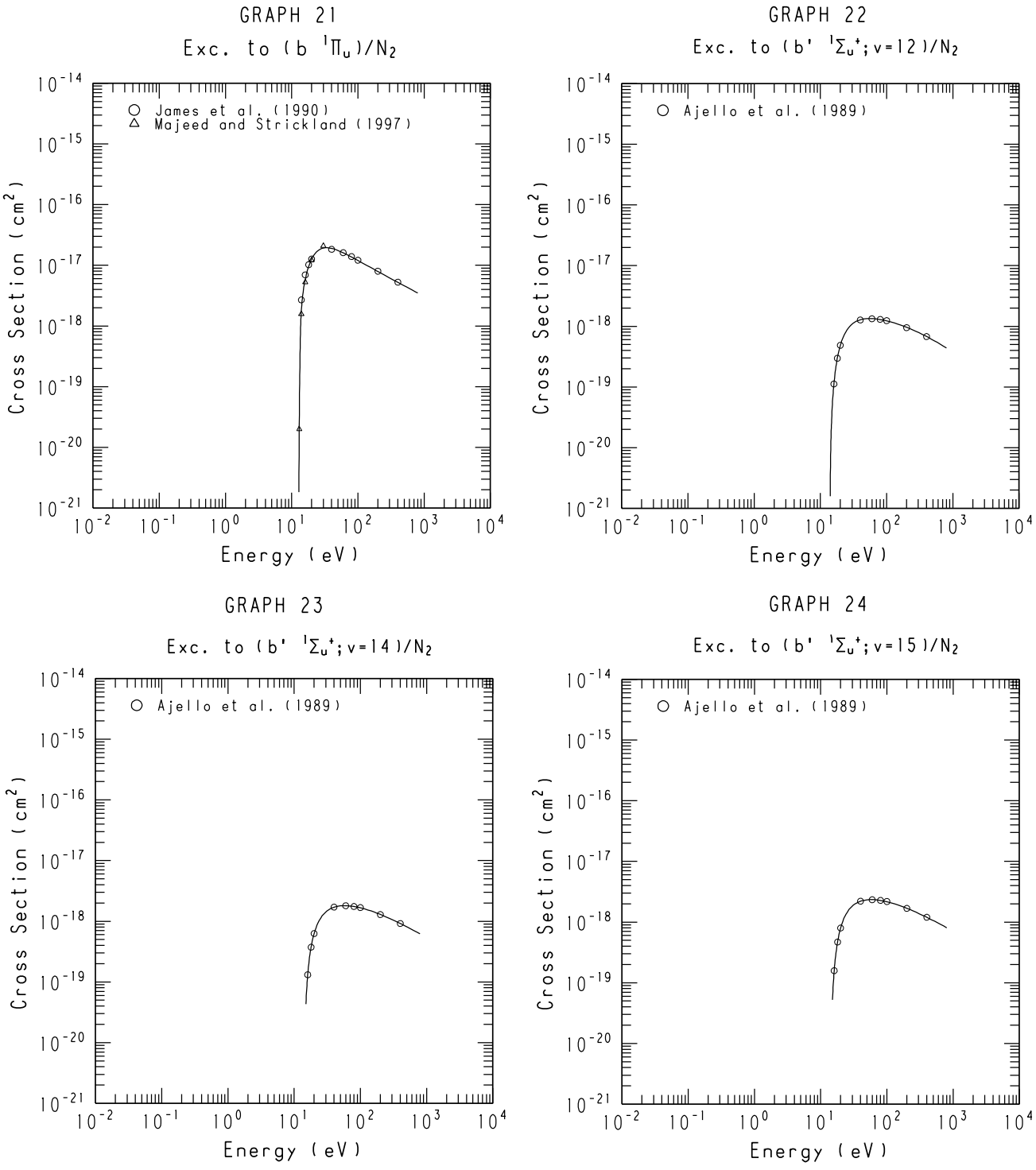

Graphs 1–75. (*continued*)

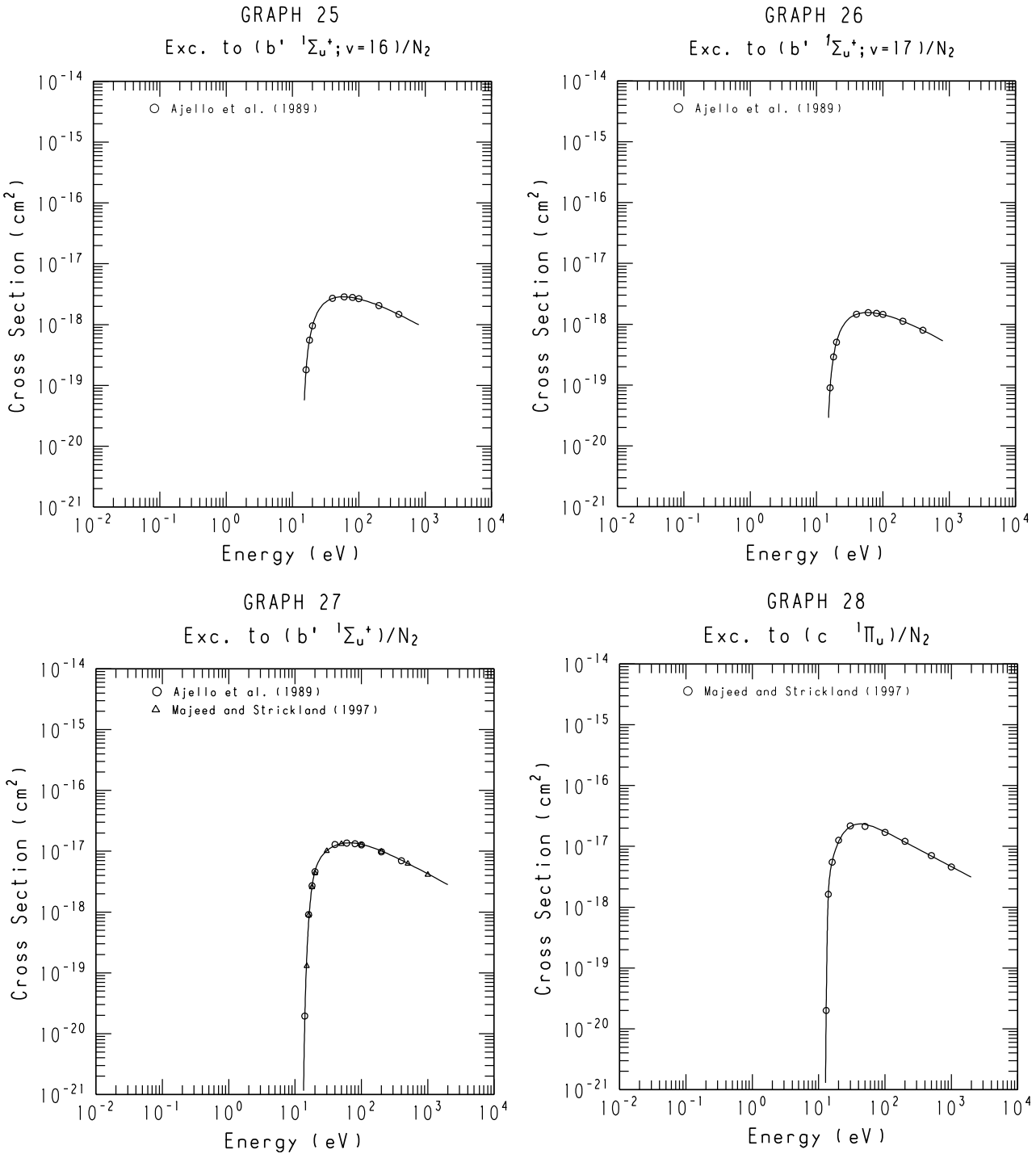

Graphs 1–75. (*continued*)

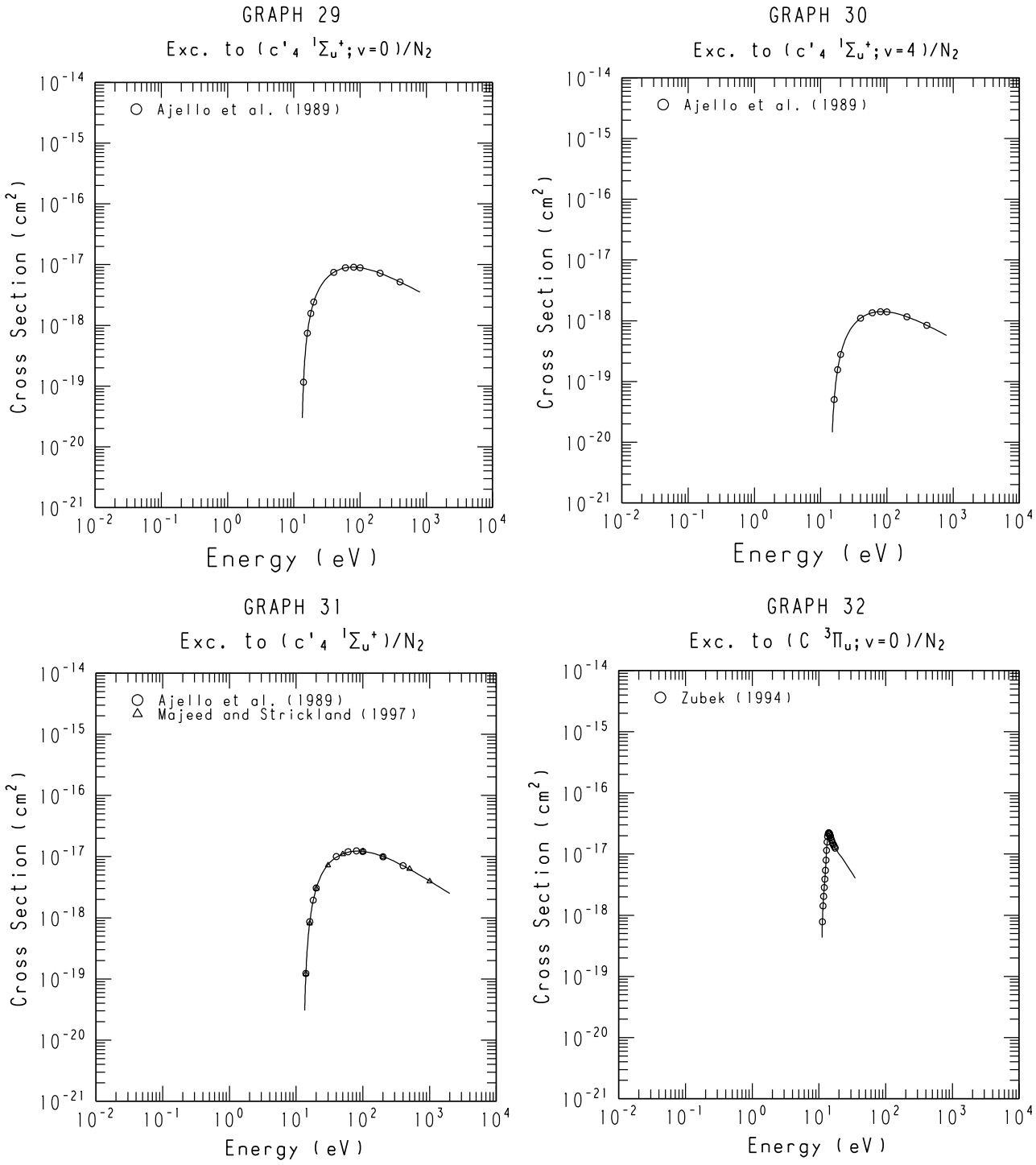

Graphs 1–75. (*continued*)

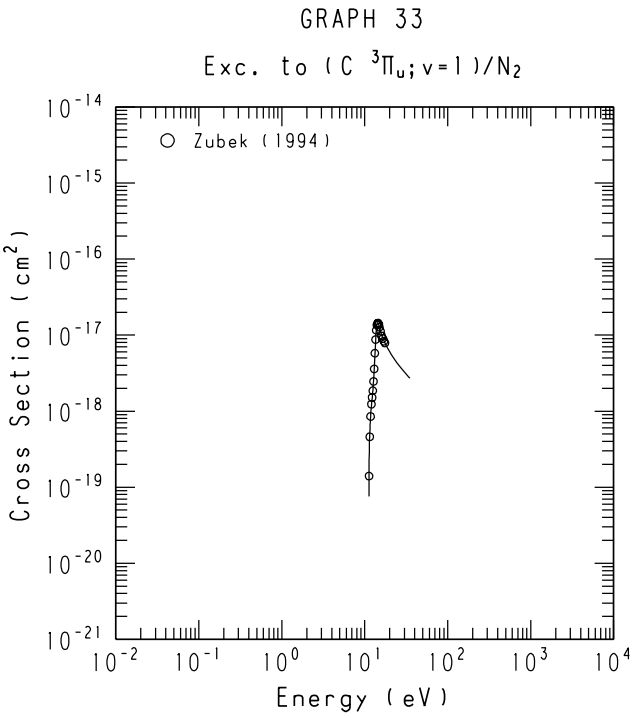

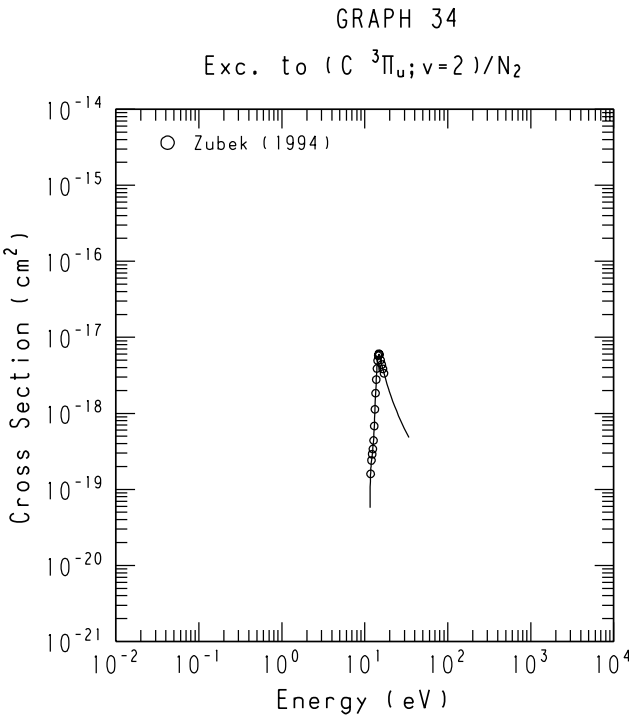

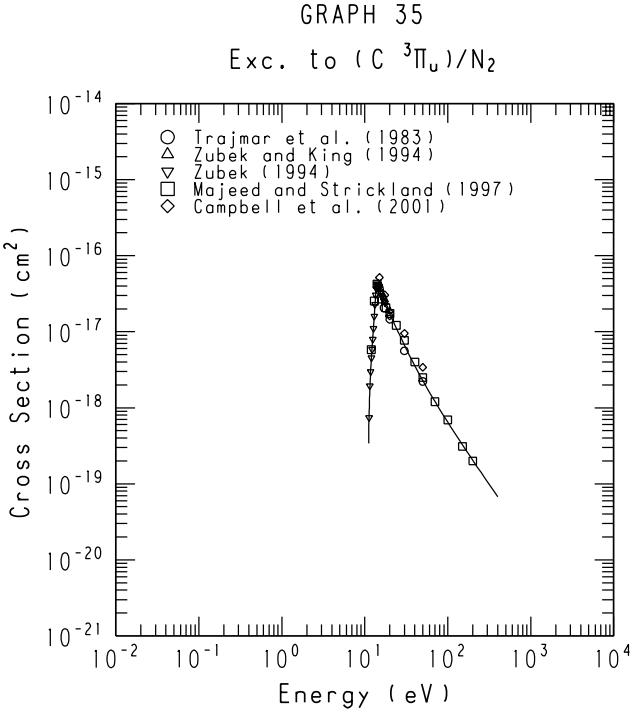

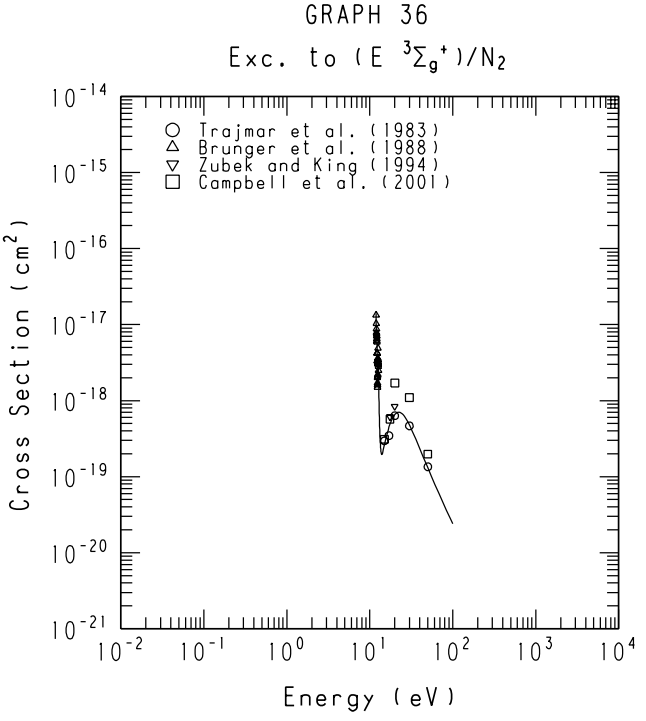

Graphs 1–75. (*continued*)

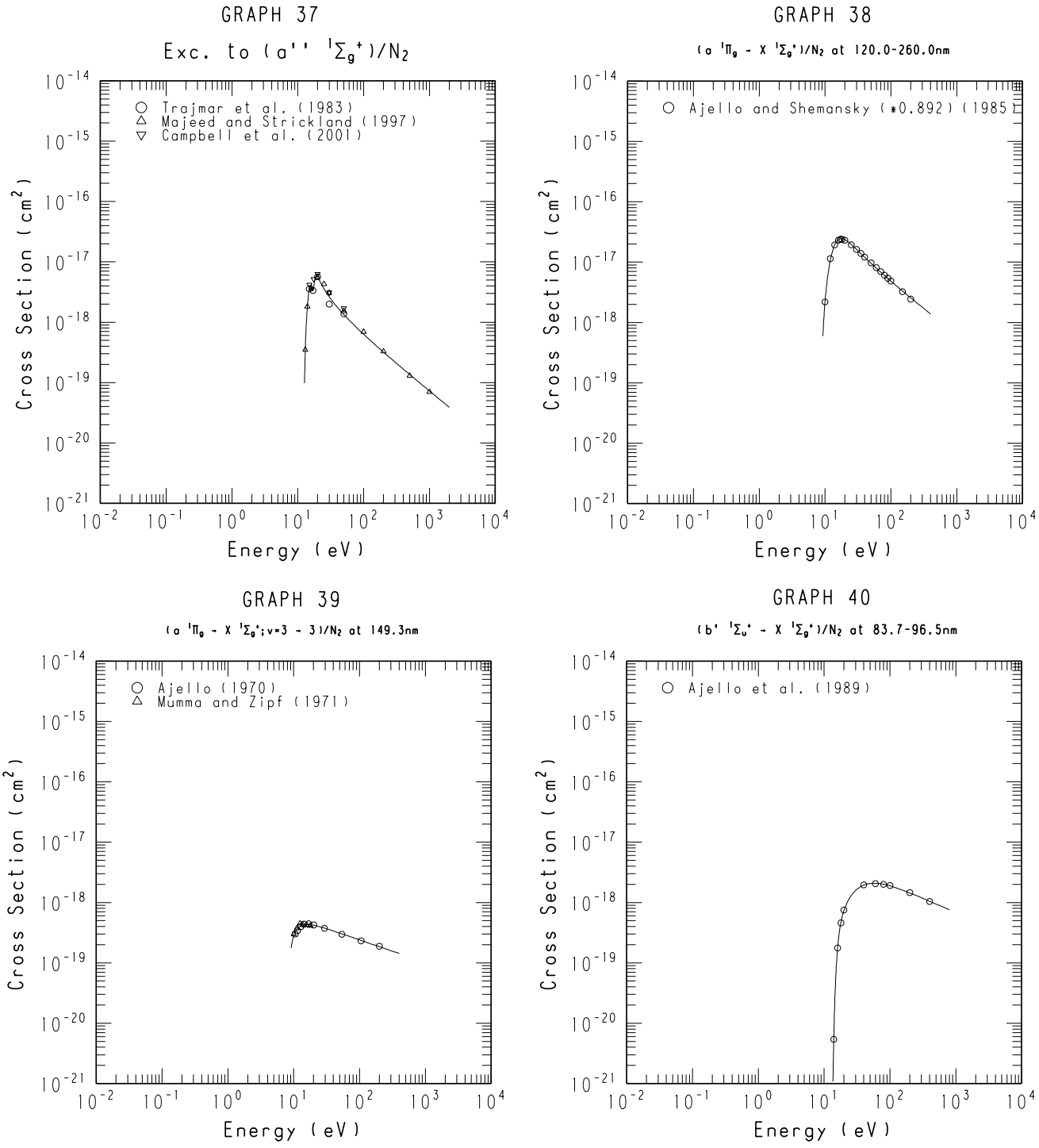

Graphs 1–75. (*continued*)

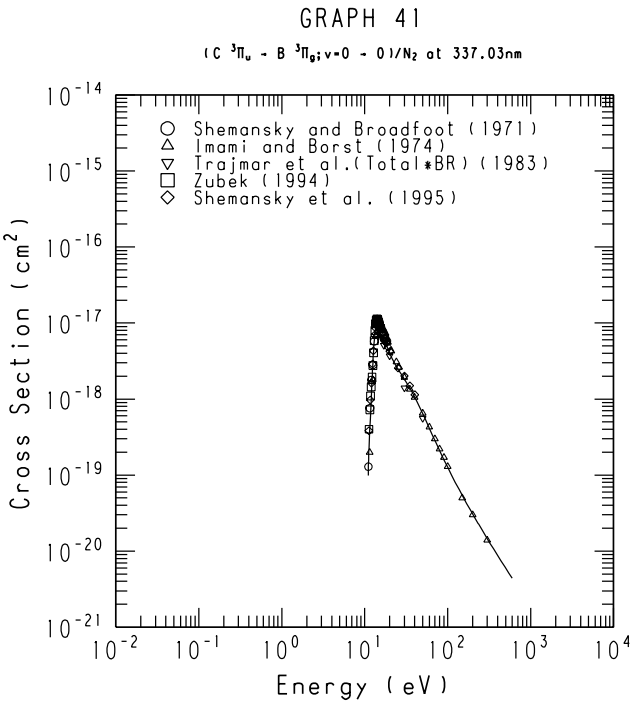

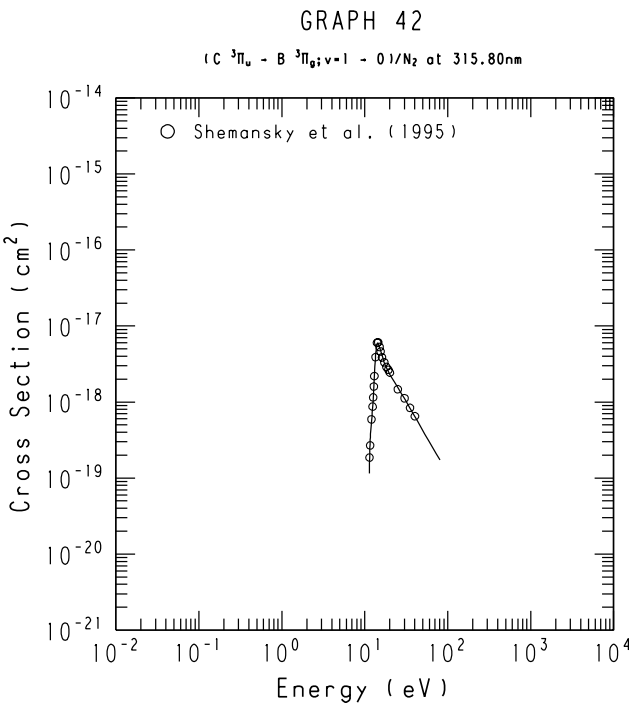

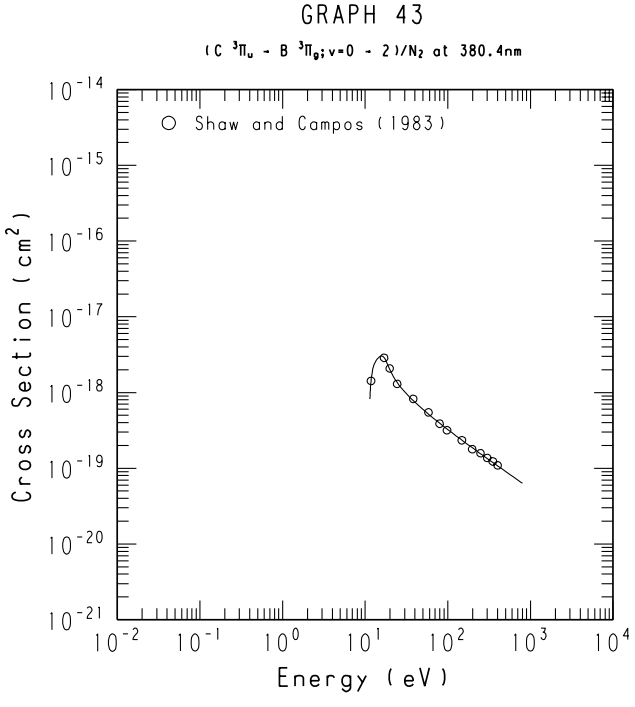

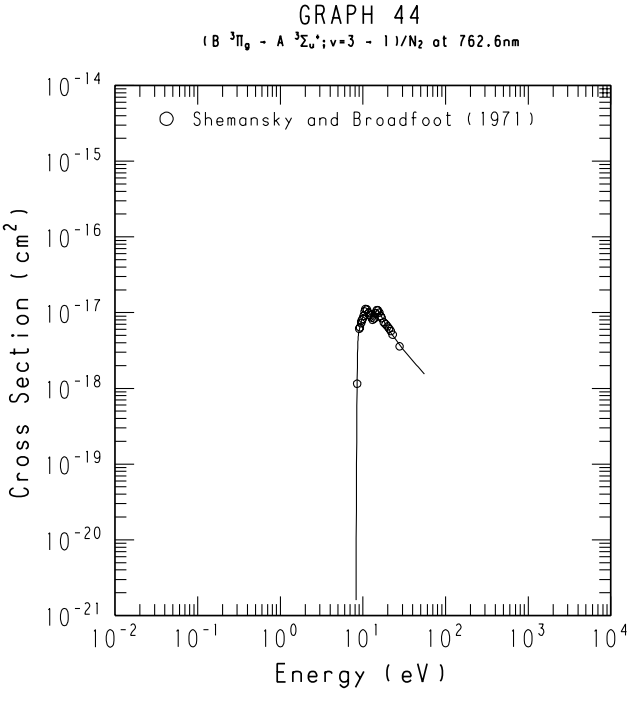

Graphs 1–75. (*continued*)

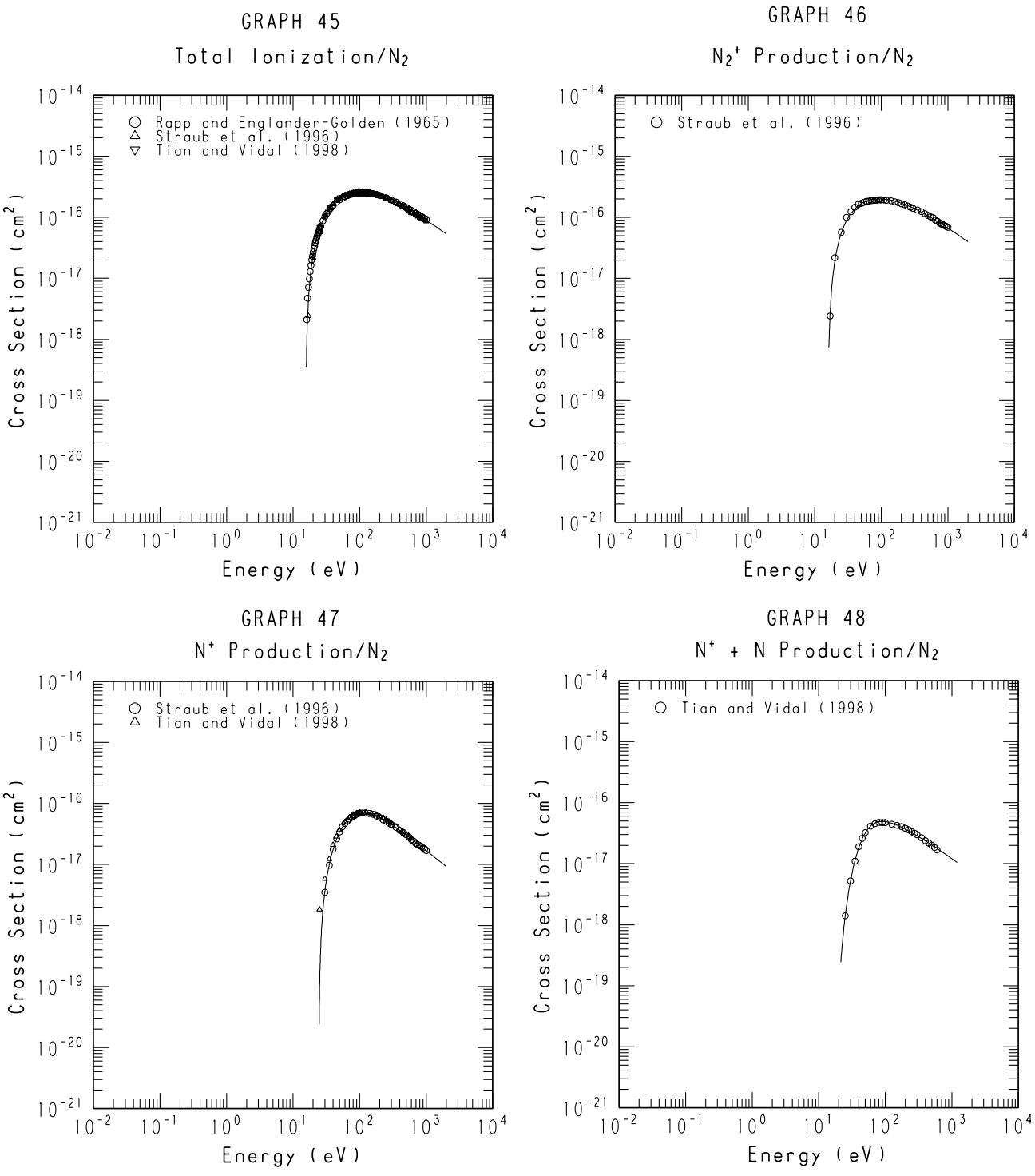

Graphs 1–75. (*continued*)

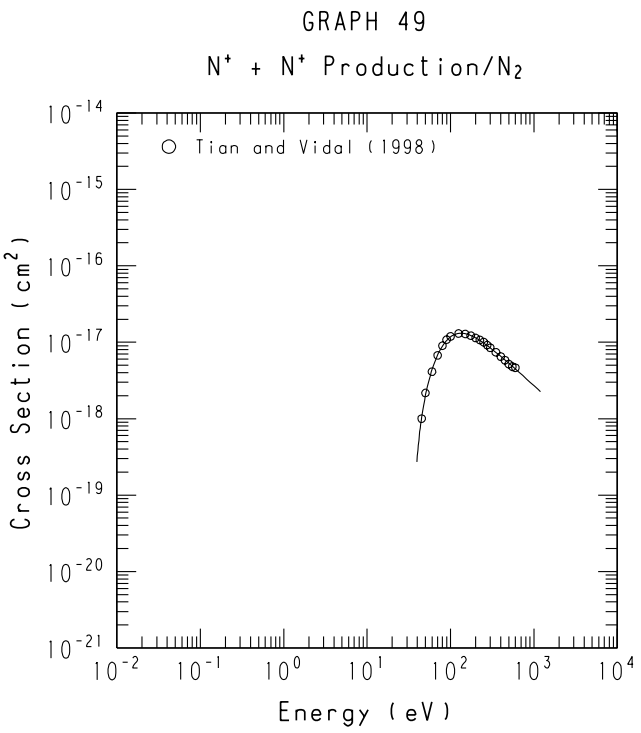

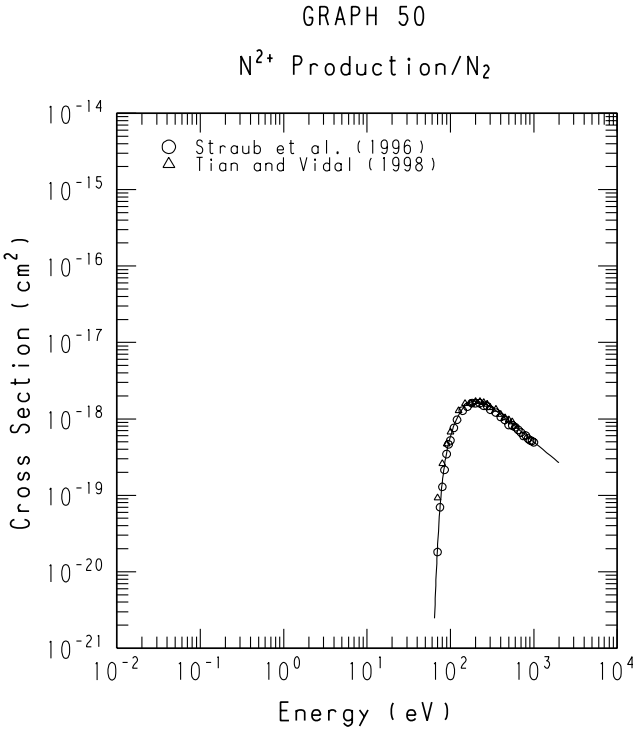

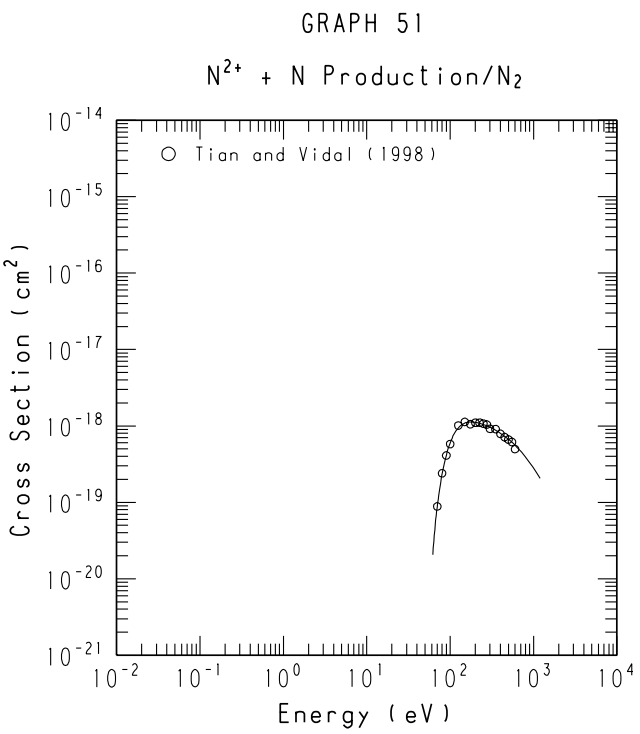

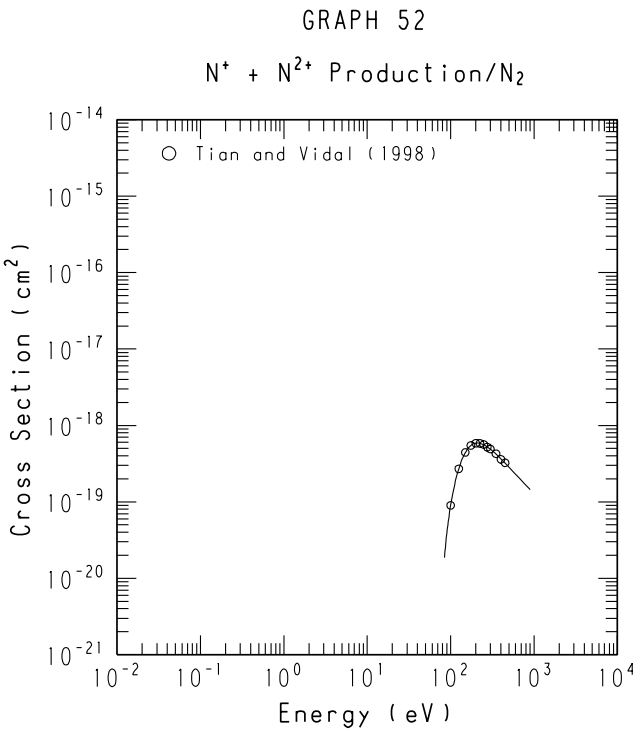

Graphs 1–75. (*continued*)

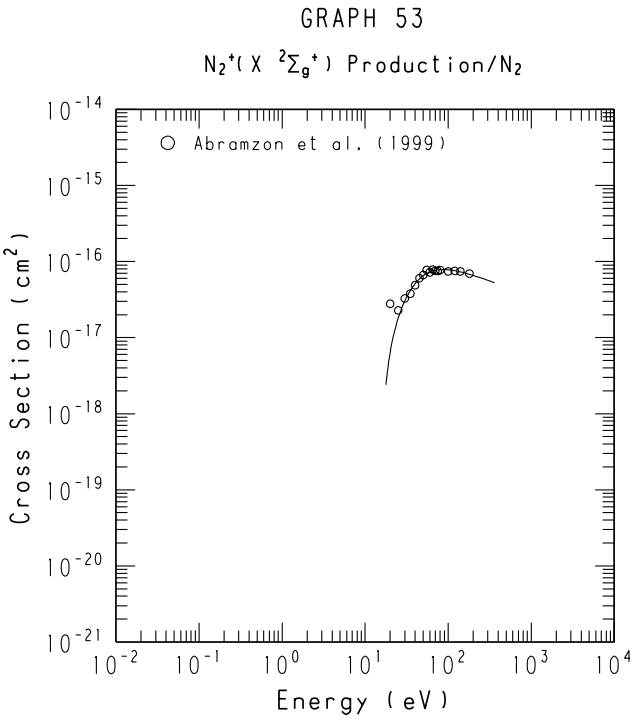

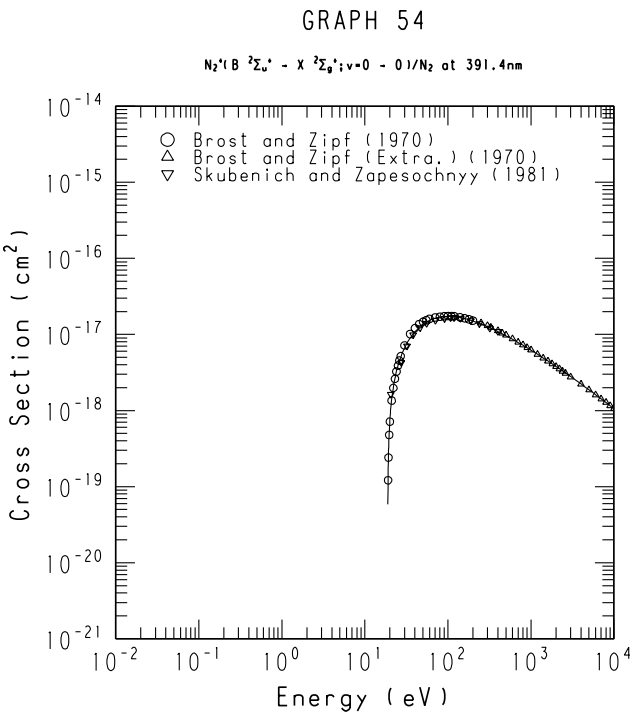

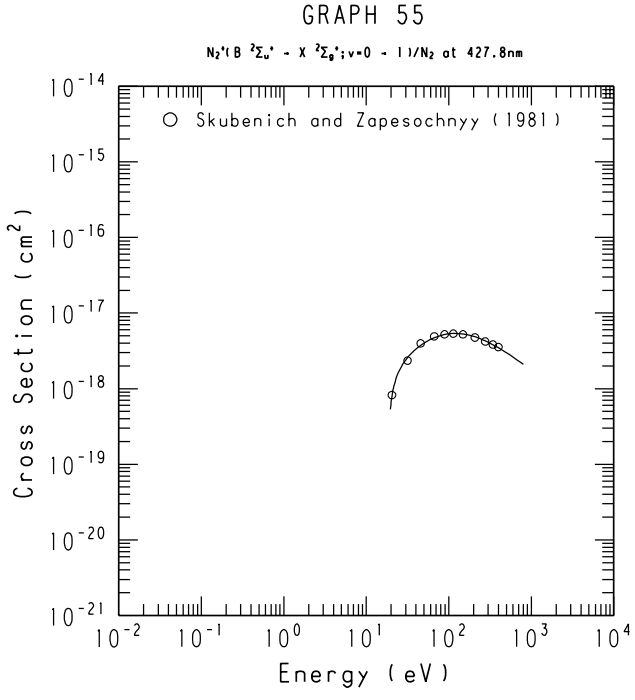

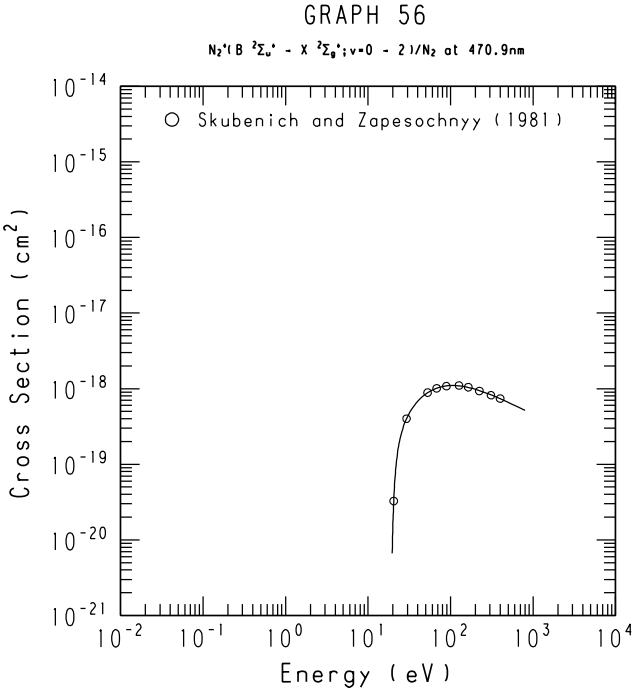

Graphs 1–75. (*continued*)

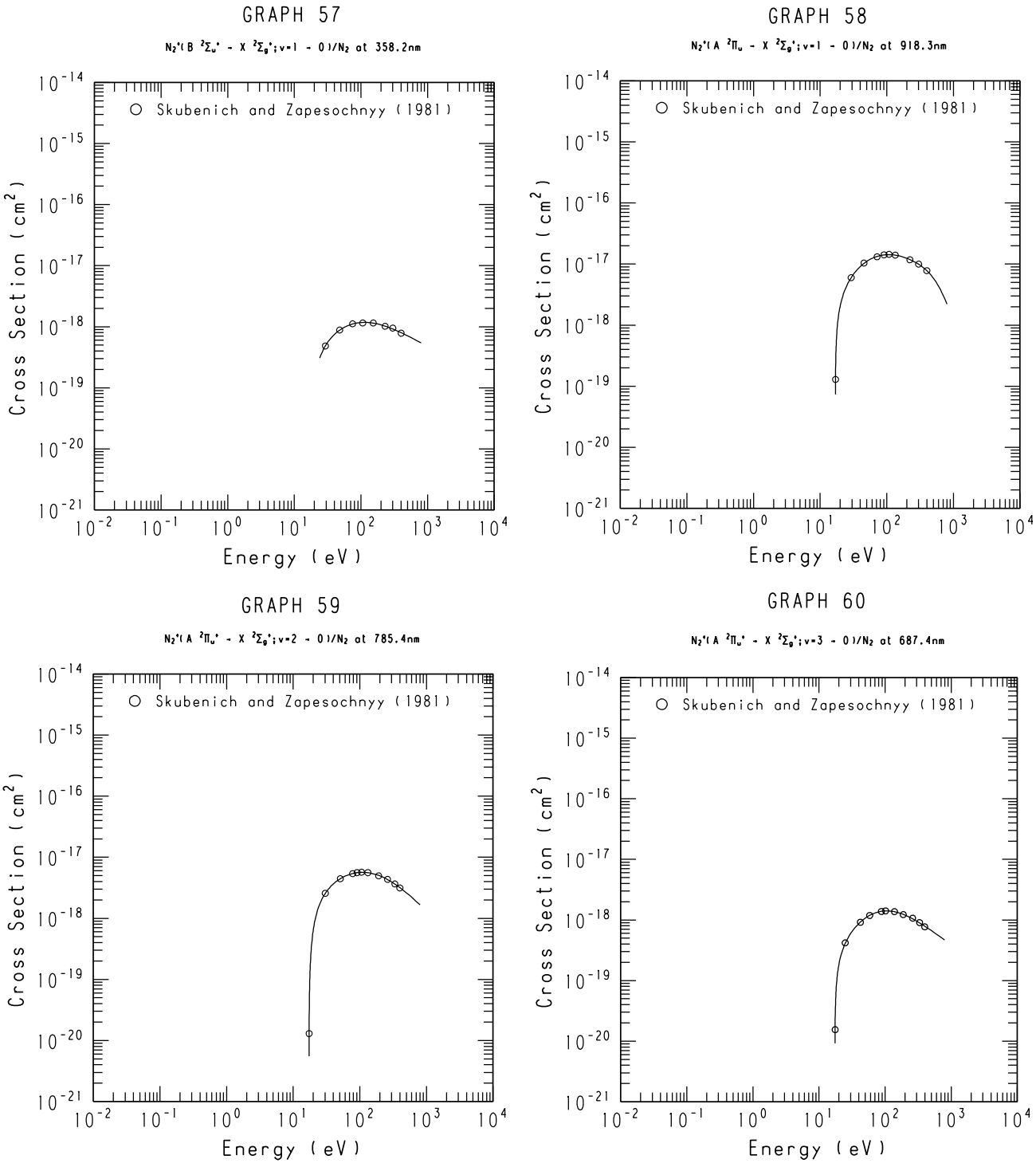

Graphs 1–75. (*continued*)

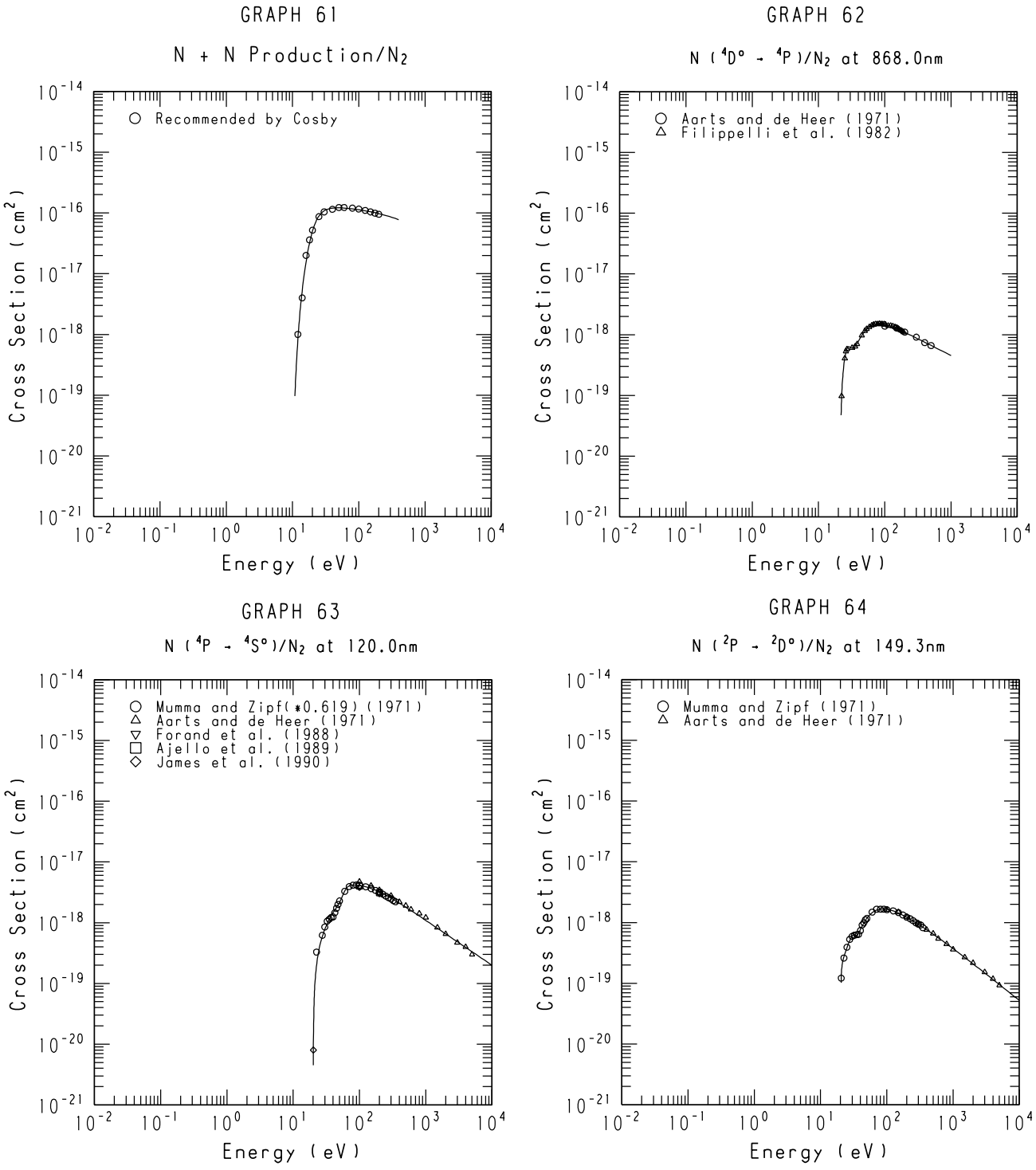

Graphs 1–75. (*continued*)

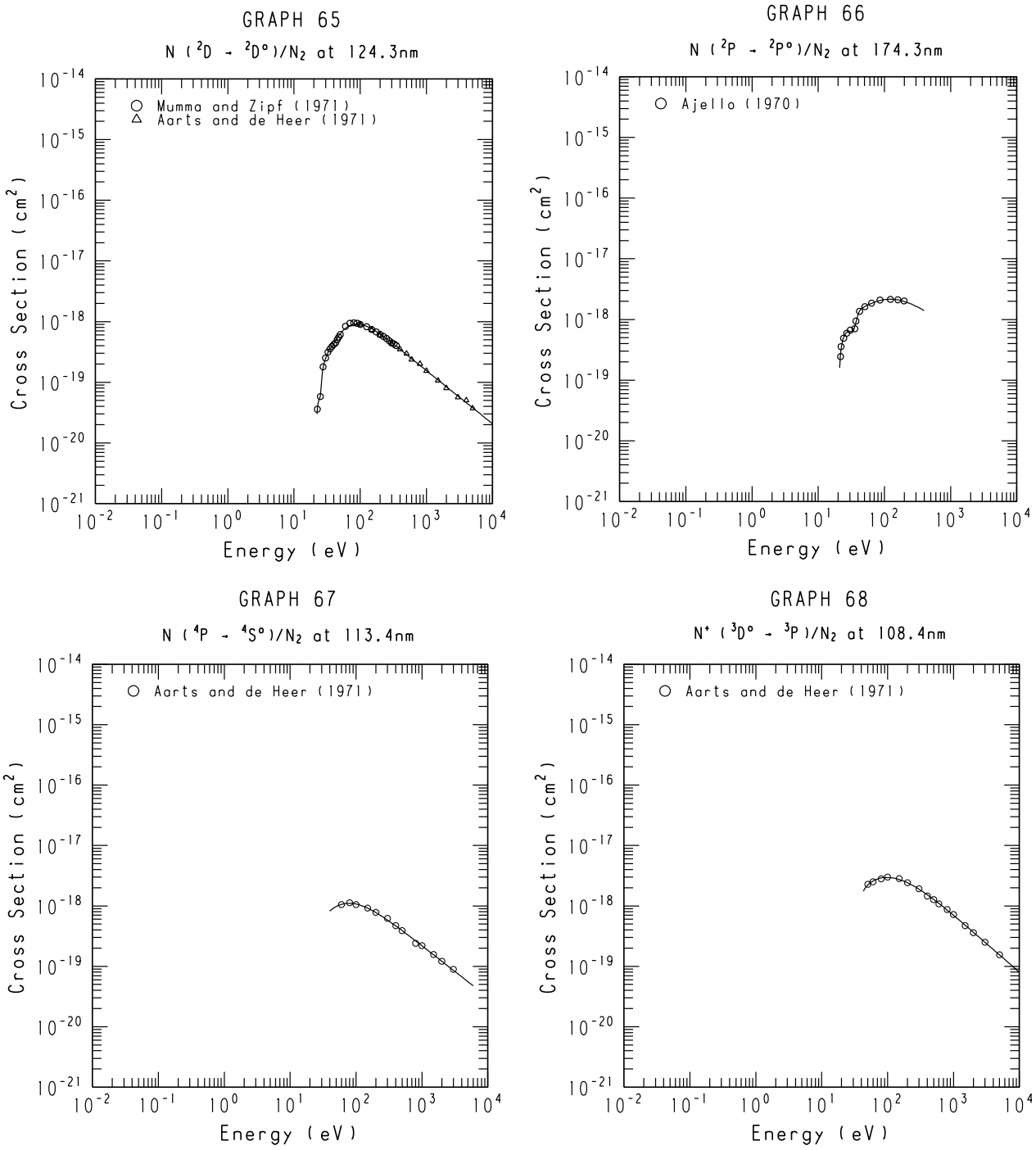

Graphs 1–75. (*continued*)

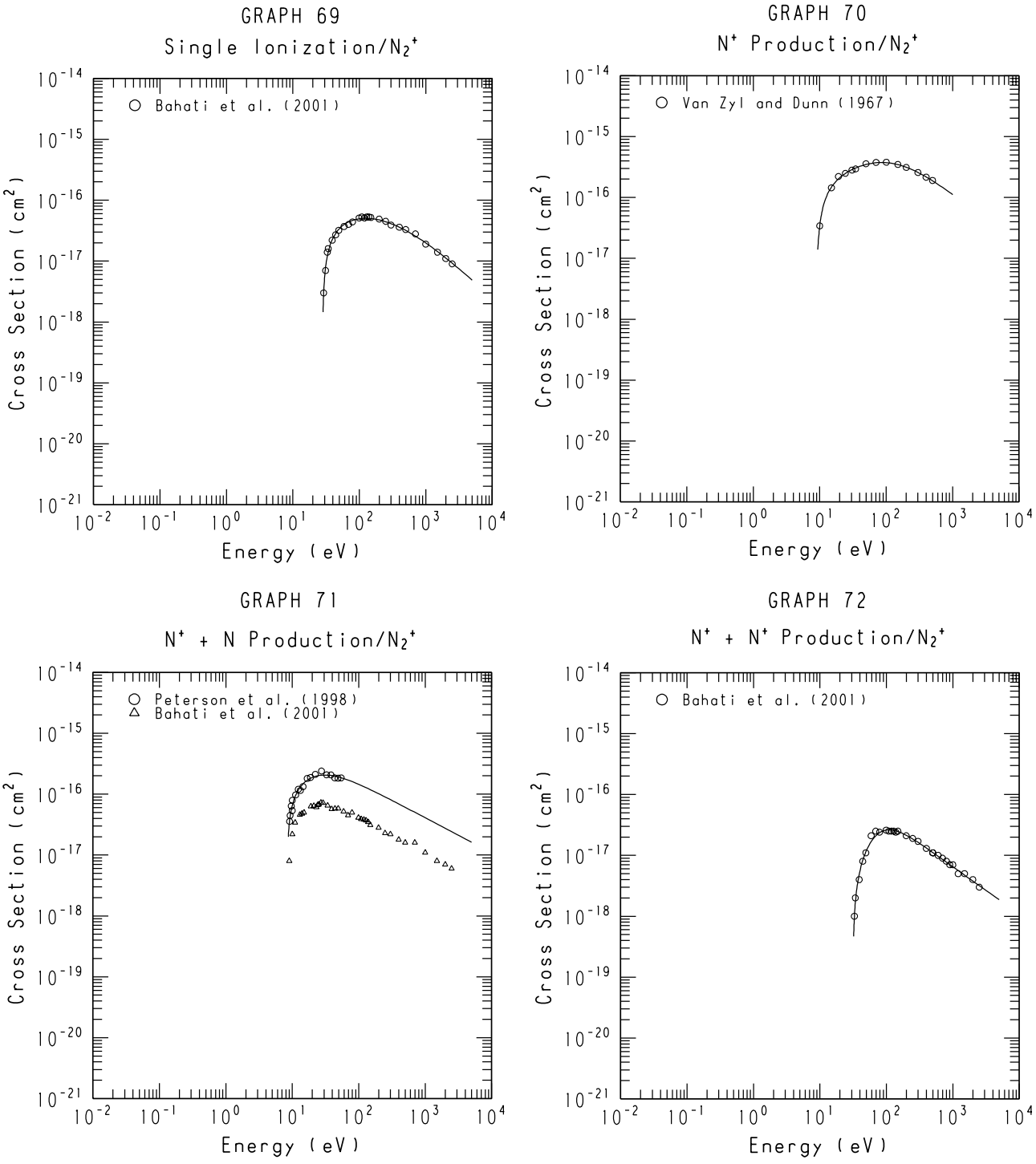

Graphs 1–75. (*continued*)

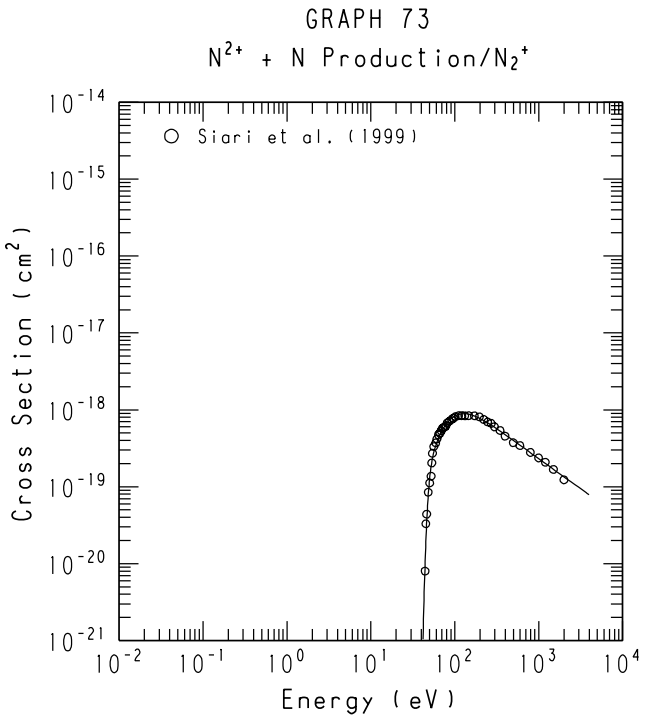

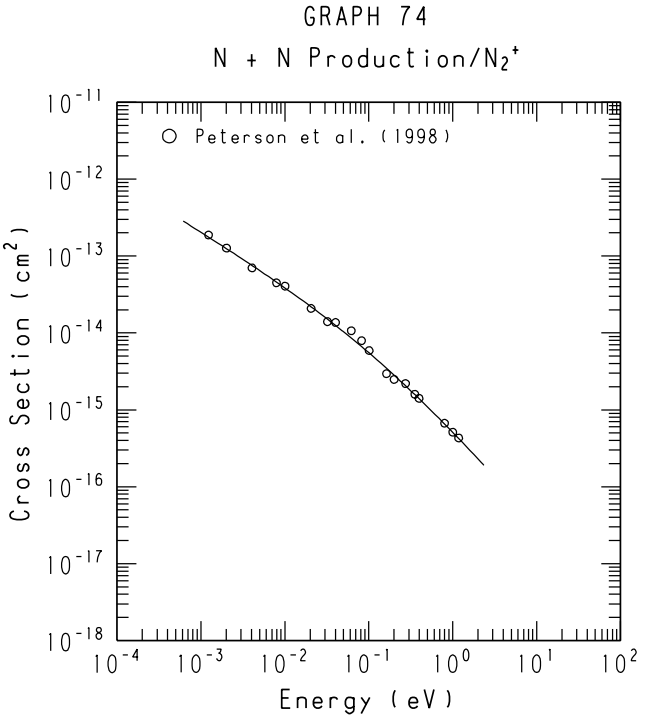

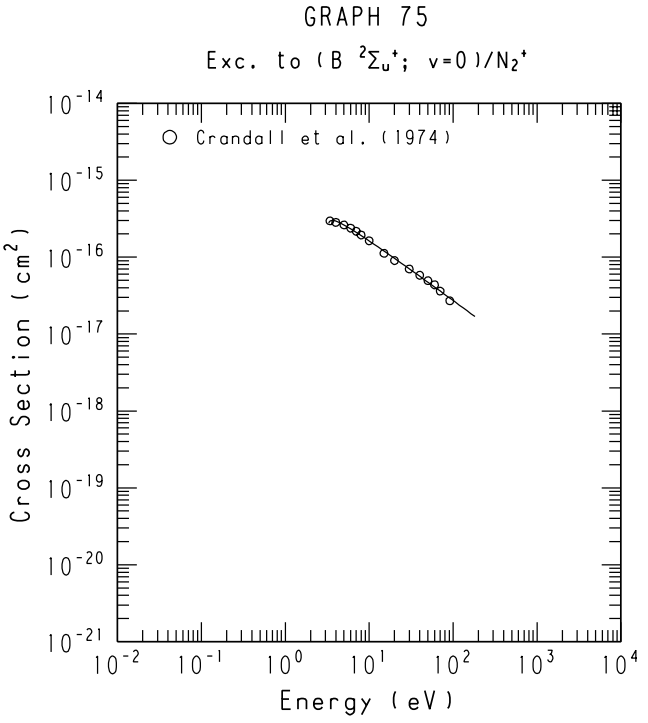

Graphs 1–75. (*continued*)